ELSEVIER

Marine Micropaleontology 29 (1996) 37–61

MARINE MICROPALEONTOLOGY

# Calcareous nannofossils as paleoproductivity indicators in Upper Cretaceous organic-rich sequences in Israel

Y. Eshet *, A. Almogi-Labin

*Geological Survey of Israel, 30 Malkhe Yisrael st., 95501, Jerusalem*

Received 20 August 1995; accepted 6 February 1996

**Abstract**

Abundant and diverse calcareous nannofossil assemblages were found in organic-rich carbonate sequences which accumulated in a Campanian–Maastrichtian upwelling belt along the southeastern Tethys. The sequences studied represent the inner (shallower) and the outer (deeper) parts of the upwelling belt. The paleoenvironmental significance of selected nannofossil taxa and their utility in productivity reconstruction was established by comparing their distribution to foraminifera and dinocyst-based productivity profiles.

Based on the calcareous nannofossil assemblages, a high-productivity group and a low-productivity group of species were determined. The distribution of these groups agrees well with the dinocyst- and foraminifera-based productivity curves and, hence, can be used to record paleoproductivity changes.

The ratio between the high-productivity and low-productivity nannofossil groups, the Nannofossil Index of Productivity (NIP), is proposed here as a productivity proxy that can be utilized in reconstructing basinal productivity development.

A quantitative analysis of the nannofossil assemblages indicates that their abundance and diversity increase towards the open sea, in the outer and less productive part of the upwelling belt. In the inner and more productive part of the upwelling belt, the nannofossils assemblages become less abundant and less diverse relative to those of the open marine environment.

*Micula decussata* and *Watznaueria barnesae* are common to abundant in most samples. *M. decussata* becomes more abundant in poorly-preserved samples. On the other hand, the distribution of *W. barnesae* matches better with intermediate productivity levels.

## 1. Introduction

Upwelling systems are characterized by their high primary productivity that is caused by the displacement of nutrient-depleted water in the photic zone by nutrient-rich subsurface water. Blooms of autotrophic phytoplankton, commonly diatomes, usually denote periods of enhanced productivity in upwelling systems (Rojas de Mandiola, 1981; Thiede and Jünger, 1992). However, diagenesis and dissolution commonly remove diatoms from pre-Quaternary sediments (Moshkovitz et al., 1983). Total organic matter in the sediment cannot be used as a measure of productivity because its preservation is largely a product of sea-floor processes (Bein et al., 1990; Pedersen and Calvert, 1990; Almogi-Labin et al., 1993). Consequently, there is a need to establish additional parameters to document productivity in places where diatoms are missing (Bralower and Thierstein, 1984, 1987). In the present study, calcare-

* Corresponding author.


*PII* S0377-8398(96)00006-0

ous nannofossil assemblages from two sections of organic-rich Campanian–Maastrichtian carbonates, which accumulated under an upwelling zone, were analyzed in order to characterize nannofossil assemblages in productive environments and to establish parameters that can help to distinguish primary productivity from the effects of sea-floor processes, such as preservation and dissolution.

The paleoenvironmental significance of calcareous nannofossils is not yet completely understood (Wise, 1982; Winter, 1985). This is partly due to the limited understanding of the functional morphology (Young, 1987, 1994) as well as the biogeography and ecology of coccolithophores (McIntyre and Bé, 1967; Okada and McIntyre, 1979; Reid, 1980; Giraudeau, 1992; Brand, 1994; Winter et al., 1994; Ziveri et al., 1995). With few exceptions (e.g. Watkins, 1989; Lamolda et al., 1992), published paleoproductivity studies concerning nannofossils relate to Tertiary or Quaternary sediments, and most of them do not identify specific significant taxa that can be used as paleoproductivity indicators. Therefore, in order to establish environmentally-significant nannofossil taxa that enable accurate productivity reconstructions, results of this study were compared with independent data from other sources: geochemistry, (Bein et al., 1990), planktic foraminifera (Almogi-Labin et al., 1993) and organic-walled dinoflagellate cysts (Eshet et al., 1994).

## 2. Previous studies

Numerous previous studies have indicated the utility of Recent to sub-Recent nannofossils in paleoenvironmental research: Roth and Berger (1975) and Winter et al. (1979) studied the distribution and environmental significance of Recent coccoliths in the Pacific and in the Red Sea, respectively. Brand (1994) described the ecology of coccolithophores, Winter et al. (1994) discussed biogeographical aspects of coccolithophore distribution in present-day oceans, and Young (1994) suggested possible relations between coccolith morphology and their ecology and living requirements. Several studies were published from marine environments of high productivity. Giraudeau (1992) analyzed Recent nannofossil assemblages deposited beneath the Benguela upwelling system (off southwestern Africa) and identified ecologically-significant taxa. Winter (1985) and Ziveri et al. (1995) studied living coccolith production in the upwelling region off southern California, where they were able to link changes in the abundance of coccoliths to seasonal changes in productivity. Backman and Chepstow-Lusty (1993), and Chepstow-Lusty and Chapman (1995) suggested the utility of *Discoasters* as indicators of low productivity in Pliocene rocks. Molfino and McIntyre (1990) and Ahagon et al. (1993) showed that *Florisphaera profunda* can be used as an indicator of enhanced productivity in Quaternary sediments.

Compared to the younger, Pliocene–Holocene fossil record, the use of older nannofossil assemblages for paleoenvironmental interpretations is problematic, mainly due to the problems of extrapolation between living and fossil taxa (e.g. Molfino and McIntyre, 1990; Young, 1994). Despite this, several studies have suggested the utility of nannofossils in interpreting the paleoenvironments of strata from Cretaceous and Jurassic intervals. Girgis (1989) made paleoenvironmental interpretations of Upper Cretaceous deposits in Egypt, based on morphometric changes in the genus *Arkhangelskiella*. Coccolith taxa that are supposed to indicate productivity changes have been identified in the mid-Cretaceous of the Atlantic and Indian Oceans (Roth and Krumbach, 1986), in the Cenomanian–Turonian (Greenhorn Formation) of the USA (Watkins, 1989) and in Albian sediments in England (Erba et al., 1992). Bralower et al. (1994) used Jurassic–Early Cretaceous nannofossil assemblages in their analysis of anoxic oceanic events. Lamolda et al. (1992) analyzed the nannofossil assemblage changes in Cenomanian sequences in England and suggested some parameters for the use of nannofossils as paleoenvironmental indicators.

The paleoenvironmental significance of Campanian–Maastrichtian sections in Israel was studied by various authors: Bartov et al. (1972), Flexer (1968) and Lewy (1990) have all proposed paleogeographic reconstructions of this time-interval in Israel. Reiss (1988) and Shemesh and Kolodny (1988) suggested that these sequences were accumulated in an upwelling regime. A recent series of geochemical and paleontological studies that focused on the Coniacian–Maastrichtian organic-rich sequences in Israel have enabled detailed reconstruction of the productivity history in these sequences (Bein et

al., 1990; Almogi-Labin et al., 1993; Eshet et al., 1994).

## 3. Geological setting

During the mid-Cretaceous, the northern Arabian plate was a passive continental margin at which Cenomanian–Turonian shelf sediments (mainly limestones, dolomites and marls) accumulated. From the Late Coniacian to the Paleocene, a new oceanographic and sedimentologic regime was established over the southeastern Tethys: transgressive conditions led to the deposition of the chalks, cherts, phosphates and organic-rich carbonates of the Menuha (Late Coniacian–Early Campanian), Mishash (Campanian), Ghareb (mainly Maastrichtian) and 'En Zetim (Campanian–Maastrichtian) Formations, all grouped within the Coniacian–Paleocene Mount Scopus Group (Flexer, 1968; Bartov et al., 1972).

During Late Coniacian–Maastrichtian times, deposition in southeastern Israel took place in tectonically-controlled NE–SW trending shelf basins, whereas open marine conditions prevailed towards the northwest. Paleogeographic reconstructions suggest that the shoreline during this period was about 100 km to the southeast during the Campanian, and even further to the east in the Maastrichtian (Bender, 1974; Germann et al., 1987; Glenn, 1990). The accumulation of organic-rich carbonates, cherts and phosphorites, as well as the microfossil assemblage composition, indicates highly productive paleoenvironments, associated with a large-scale upwelling system that existed along the southern margins of the Tethys (Reiss, 1988; Almogi-Labin et al., 1993; Eshet et al., 1994).

Both sections studied (Fig. 1) are characterized by organic-rich carbonates (12–13% average Total Organic Matter, TOM). They belong to two of the main lithofacies types described for the Mount Scopus Group in Israel by Flexer (1968) and Bartov et al. (1972): the Shefela section (Shefela Basin) belongs to the marly-chalky Zefat lithofacies, representing the outer shelf and upper slope, and the Zin section (Zin Basin) belongs to the Zin lithofacies of alternating organic-rich carbonates, cherts, phosphorites, marls and porcelanites, representing the more restricted inner shelf basins in the southeastern part of Israel (Flexer, 1968; Bartov et al., 1972).

## 4. Biostratigraphy

Biozonation of the studied sections (Fig. 1) is based on planktic foraminifera (Almogi-Labin et al., 1993) and calcareous nannofossils (Eshet and Moshkovitz, 1995). The nannofossil zonation used in the present paper is based on the NC zonation scheme of Roth (1978) because it suits the Israeli nannofossil assemblages better than the CC zonation of Sissingh (1977), as shown by Eshet and Moshkovitz (1995). The Shefela section ranges from the Late Campanian *Quadrum sissinghii* nannofossil Zone (= NC19b) to the Late Maastrichtian *Lithraphidites quadratus* nannofossil Zone (= NC22). It is equivalent to the interval between the *Globotruncana rosetta* and the *Abathomphalus mayaroensis* planktic foraminifera zones (Fig. 1). The Zin section ranges from the late Early Campanian (*Ceratolithoides aculeus* Zone) into the Early Maastrichtian (*Q. trifidum* Zone). It is equivalent to the interval between the *Globotruncana rosetta* and the *G. falsostuarti* planktic foraminifera zones.

Three distinct stratigraphic datum levels (marked by the letters A, B and C in all text figures) were used to correlate between the sections:

(A) The top of the Main Chert Member of the Mishash Formation (Campanian);

(B) The first occurrence (FO) of the coccolith *Quadrum trifidum* (Late Campanian);

(C) The FOs of the Maastrichtian planktic foraminifers *Globotruncana falsostuarti* and *Gansserina wiedenmayeri*, and the benthic foraminifer *Siphogenerinoides parva* (Campanian–Maastrichtian boundary). In previous works, these datums have been found useful for correlation (e.g. Reiss et al., 1985; Gvirtzman et al., 1989; Almogi-Labin et al., 1993).

## 5. Materials and methods

The present study is based on the quantitative analysis of calcareous nannofossils assemblages in 84 Campanian–Maastrichtian core samples: 29 from two adjacent cores (Hartuv B and Zor'a B) in the Shefela Basin, Israeli coastal plain, and 57 samples from the Saraf core section in the Zin Basin, Negev, southern Israel (Fig. 1). The same samples were previously used to determine the paleoproductivity history of the basins, based on geochemistry

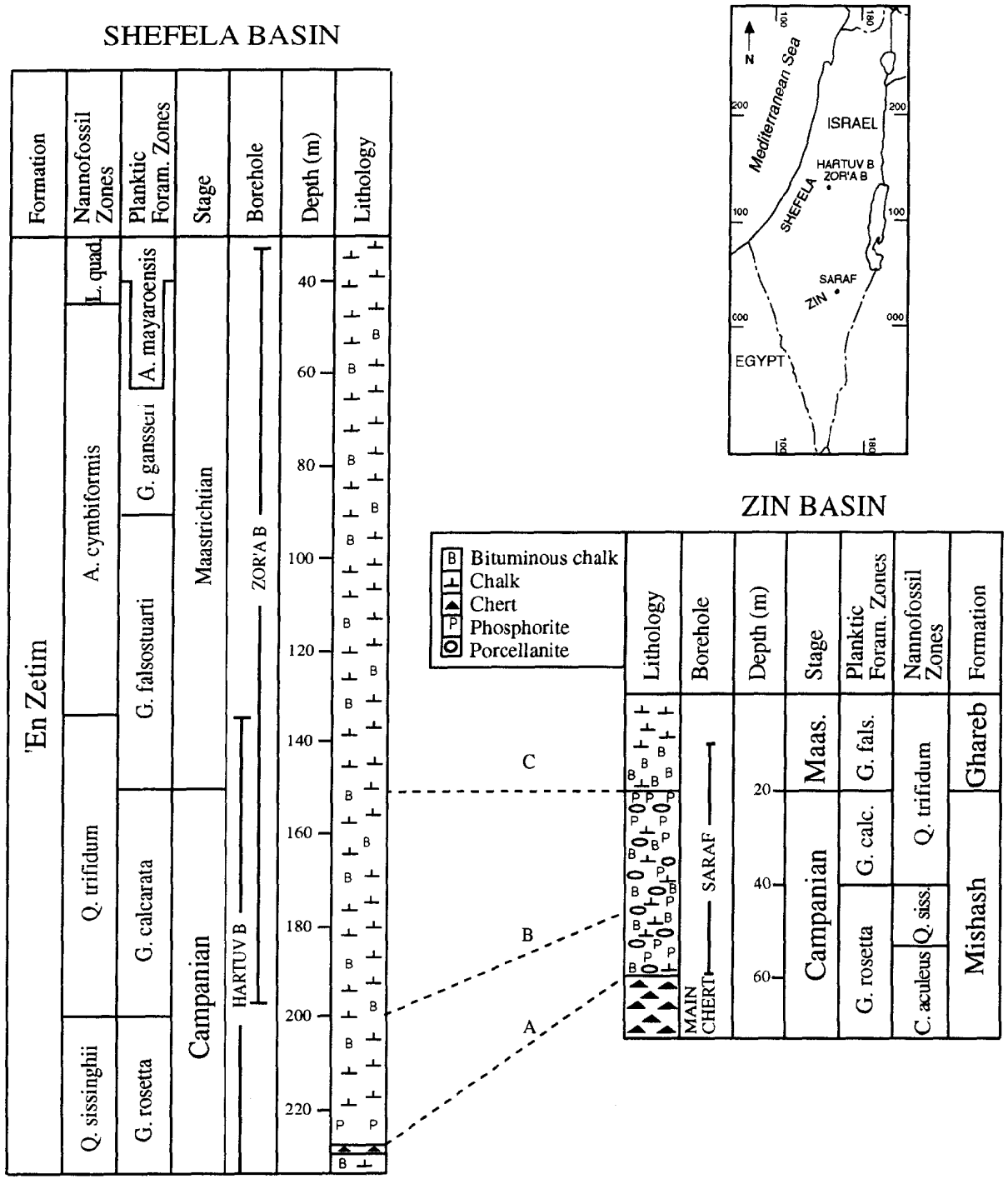


Fig. 1. Litho- and biostratigraphic correlation between the studied sections. A = top of Main Chert; B = first occurrence of *Quadrum trifidum*; C = base Maastrichtian (first occurrence of *Gansserina wiedenmayeri* and *Siphogenerinoides parva*). Calcareous nannofossil zonation follows the NC scheme of Roth, 1978, according to Eshet and Moshkovitz (1995).

(Bein et al., 1990), benthic and planktic foraminifera (Almogi-Labin et al., 1993) and dinoflagellate cysts (Eshet et al., 1994). The cherty interval between 60 and 70 m (Main Chert unit in Fig. 1) could not be processed for calcareous nannofossils. The cores and the samples are deposited at the Geological Survey of Israel, Jerusalem.

Nannofossil slides for light microscope study were prepared following a suspension method (separation of the heavy fraction after one minute in suspension, and concentration of the suspended material after 15 minutes of settling in distilled water). A 10% solution of sodium hypochlorite (NaOCl, bleach) was used to oxidize and dissolve the organic matter prior to slide preparation in order to improve the visibility of fossils under the microscope (Eshet, 1996).

Nannofossil abundance and species diversity were based on counting a population of 300 specimens per sample. Since all samples were prepared similarly, it is suggested that these counts can be used to approximate the nannofossil assemblages. Abundance was estimated using the parameter Nannofossils per Visual Field (NVF of Florés, 1992). The quantitative analysis of nannofossils in the present study included only species that make up more than 1% of the sample. Minor species, that make up less than 1% were included only in the species diversity counts. The complete semi-quantitative distribution of all taxa in the studied sections was given by Eshet and Moshkovitz (1995). Preservation of the nannofossil assemblage is indicated as the percentage of whole nannofossils in the assemblage (Figs. 2 and 3). Comparative data on the preservation of foraminifers is only available for the Shefela section. The degree of planktic foraminifera preservation is expressed as the percentage of broken foraminifers in the entire assemblage.

The nannofossil-derived productivity profiles are compared with profiles from planktic foraminifera and dinocysts as follows: the planktic foraminifera-derived productivity reconstruction was obtained by classifying the assemblages into four groups (P-Types of Almogi-Labin et al., 1993), ranging from Type 1 (lower productivity) to Type 4 (highest productivity). Each group was defined by abundance and species diversity, as well as by the presence of specific indicative taxa (Figs. 2 and 3). The dinoflagellate-based productivity reconstruction (P/G ratio in Figs. 2 and 3) is the value of the ratio between the predominating dinocyst groups (the presumably heterotrophic peridinioids and the autotrophic gonyaulacoids), where productivity increases from a low to a high P/G value (Powell et al., 1990; Eshet et al., 1994).

Varimax factor analysis (Davis, 1973) was carried out on species and taxa comprising $\geq 1\%$ of the assemblage, on the two ecological groups, and on several geochemical and independent productivity-related paleontological parameters, using the STATISTICA© software package, StatSoft, Release 5.0.

## 6. Results

Seventy two nannofossil taxa were identified in the present study. Most samples contain a rich and diverse flora with *Watznaueria barnesae* and *Micula decussata* as the most prominent taxa. For the complete taxonomic list and distribution charts, see Eshet and Moshkovitz (1995). In some intervals, a 'nannofossil ooze' was found. Some horizons are characterized by the predominance of a limited number of species that form almost 'monospecific' nannofossil assemblages, e.g. Shefela section, samples HRB 26 and ZRB 9, where *Micula decussata* constitutes almost 70% of the assemblage (Plate I, 14). Some taxa exhibit a great size-range, among them *Arkhangelskiella cymbiformis*, *Kamptnerius magnificus* and *Gartnerago obliquum*. The significance of this size-variation has not been investigated in the present paper, but as suggested by Girgis (1989), it may reflect environmental changes. The possibility that these variations reflect productivity changes should not be ignored in future studies.

### *6.1. Productivity proxies and the nannofossil assemblages*

The following results were obtained for total organic matter, foraminifera- and dinocyst-based productivity proxies, as well as nannofossil abundance, diversity and preservation:

**Shefela section** (Fig. 2; Table 1): TOM is quite uniform throughout the section, with low values at the top (above 50 m) and higher values at the base (below 225 m). Independently derived foraminifera-

Table 1
Nannofossil counts in the Shefela section. SPC. DIV = Species Diversity; NVF = Nannofossils per Visual Field; PRES. = Preservation; M. DEC. = *Micula decussata*; W. BAR = *W. barnesae*; T. OPER. = *Thoracosphaera operculata*; E. TURR. = *E. turriseiffelii*; PRED. = *Prediscosphaera*; LITHR SPP. = *Lithraphidites* spp.; VEK. & VAG. = *Vekshinella* and *Vagalapilla*; GLAUK. = *Glaukolithus*; BISC. = *Biscutum*; T. SAX. = *Thoracosphaera saxea*. Low PROD. = low productivity; High PROD. = high productivity; NIP = Nannofossil Index of Productivity. Sample 18 is cherty and has no nannofossils

| Sam. no. | Depth m | $CaCO_3$ % | TOM % | P/G | LOG P/G | P-TYPE | SPC. DIV | NVF | PRES. % | M. DEC. | W. BAR | T. OPER. | E. TURR. | PRED. | LITHR SPP. | VEK. & VAG. | GLAUK SPP. | BISC SPP. | T. SAX | Low PROD. | High PROD. | NIP | Others % |
|---|---|---|---|---|---|---|---|---|---|---|---|---|---|---|---|---|---|---|---|---|---|---|---|
| 3 | 33.2 | 86 | 0 | 0.08 | −1.097 | 1 | 31 | 52 | 63 | 8 | 19 | 14 | 6 | 3 | 8 | 3 | 1 | 0 | 0 | 34 | 1 | −1.53 | 38 |
| 4 | 45.2 | 63 | 8 | 0.88 | −0.056 | 2 | 21 | 41 | 47 | 22 | 17 | 15 | 4 | 2 | 6 | 4 | 1 | 0 | 0 | 31 | 1 | −1.49 | 29 |
| 5 | 46.0 | 51 | 11 | 1.5 | 0.176 | 1.5 | 34 | 42 | 44 | 27 | 25 | 6 | 4 | 3 | 5 | 3 | 2 | 2 | 1 | 21 | 5 | −0.62 | 22 |
| 6 | 51.0 | 47 | 12 | 1.25 | 0.097 | 2 | 28 | 40 | 37 | 10 | 30 | 7 | 3 | 2 | 6 | 2 | 2 | 3 | 1 | 20 | 6 | −0.52 | 34 |
| 7 | 54.7 | 52 | 11 | 0.04 | −1.398 | 1 | 32 | 48 | 31 | 58 | 7 | 10 | 4 | 4 | 6 | 3 | 1 | 0 | 0 | 27 | 1 | −1.43 | 7 |
| 8 | 60.0 | 58 | 10 | 0.02 | −1.699 | 1 | 31 | 44 | 62 | 16 | 41 | 12 | 3 | 3 | 5 | 2 | 1 | 0 | 0 | 25 | 1 | −1.40 | 17 |
| 9 | 68.0 | 60 | 11 | 0.08 | −1.097 | 1 | 29 | 49 | 24 | 64 | 8 | 3 | 3 | 1 | 4 | 1 | 0 | 0 | 0 | 12 | 0 | | 16 |
| 10 | 84.0 | 58 | 10 | 0.75 | −0.125 | 1.5 | 29 | 44 | 31 | 44 | 25 | 8 | 5 | 2 | 5 | 2 | 2 | 2 | 0 | 22 | 4 | −0.74 | 5 |
| 11 | 102.5 | 79 | 5 | 1.5 | 0.176 | 3 | 23 | 34 | 33 | 19 | 34 | 8 | 4 | 3 | 4 | 3 | 4 | 4 | 2 | 22 | 10 | −0.34 | 15 |
| 12 | 108.5 | 53 | 17 | 2 | 0.301 | 3.5 | 18 | 40 | 28 | 41 | 12 | 5 | 2 | 2 | 3 | 1 | 8 | 7 | 4 | 13 | 19 | 0.16 | 15 |
| 35 | 133.0 | 62 | 14 | 0.85 | −1.301 | 2 | 21 | 45 | 58 | 9 | 19 | 8 | 4 | 3 | 5 | 3 | 4 | 4 | 2 | 23 | 10 | −0.36 | 39 |
| 13 | 138.0 | 67 | 20 | 1.2 | 0.079 | 2 | 18 | 46 | 52 | 10 | 36 | 7 | 4 | 3 | 4 | 3 | 4 | 5 | 2 | 21 | 10 | −0.32 | 22 |
| 34 | 141.0 | 61 | 12 | 6 | 0.778 | 4 | 18 | 41 | 37 | 21 | 45 | 2 | 3 | 1 | 2 | 2 | 10 | 7 | 4 | 10 | 21 | 0.32 | 3 |
| 14 | 144.0 | 70 | 19 | 5 | 0.699 | 4 | 17 | 35 | 42 | 10 | 33 | 3 | 2 | 0 | 2 | 2 | 12 | 8 | 5 | 9 | 25 | 0.44 | 23 |
| 33 | 147.0 | 54 | 11 | 3 | 0.477 | 3 | 17 | 30 | 43 | 10 | 48 | 4 | 1 | 1 | 3 | 1 | 9 | 7 | 3 | 10 | 19 | 0.28 | 13 |
| 25 | 149.0 | 64.3 | 12 | 3.5 | 0.544 | 3.0 | 21 | 45 | 55 | 12 | 35 | 3 | 1 | 1 | 2 | 3 | 8 | 6 | 3 | 10 | 17 | 0.23 | 26 |
| 32 | 152.0 | 55 | 17 | 2.5 | 0.398 | 3.0 | 15 | 10 | 34 | 20 | 51 | 2 | 1 | 1 | 1 | 0 | 11 | 7 | 2 | 5 | 20 | 0.60 | 4 |
| 24 | 154.0 | 73.4 | 8.2 | 2.5 | 0.398 | 3 | 21 | 43 | 68 | 10 | 40 | 5 | 2 | 1 | 2 | 3 | 10 | 8 | 3 | 10 | 21 | 0.32 | 16 |
| 23 | 158.0 | 71.4 | 11 | 3.5 | 0.544 | 3.0 | 21 | 35 | 62 | 13 | 38 | 3 | 1 | 1 | 3 | 2 | 10 | 9 | 4 | 10 | 23 | 0.36 | 16 |
| 31 | 174.0 | 71 | 15 | 6 | 0.778 | 4.0 | 21 | 34 | 53 | 10 | 30 | 2 | 2 | 2 | 4 | 1 | 8 | 10 | 5 | 11 | 23 | 0.32 | 26 |
| 30 | 184.0 | 70 | 12 | 3.5 | 0.544 | 3.0 | 21 | 38 | 56 | 11 | 39 | 8 | 4 | 3 | 6 | 1 | 5 | 4 | 4 | 22 | 13 | −0.23 | 15 |
| 29 | 191.0 | 63 | 13 | 0.9 | −0.046 | 2.0 | 23 | 40 | 48 | 10 | 41 | 10 | 5 | 5 | 4 | 2 | 3 | 2 | 2 | 31 | 7 | −0.65 | 16 |
| 15 | 197.0 | 61 | 10 | 5 | 0.699 | 1.0 | 27 | 53 | 62 | 4 | 38 | 13 | 6 | 5 | 6 | 3 | 2 | 0 | 0 | 33 | 2 | −1.22 | 23 |
| 28 | 201.0 | 49 | 10 | 0.04 | −1.398 | 1.0 | 23 | 47 | 64 | 4 | 11 | 12 | 4 | 4 | 4 | 2 | 3 | 0 | 0 | 28 | 3 | −0.97 | 56 |
| 27 | 212.0 | 53 | 16 | 1 | 0.000 | 2.0 | 17 | 14 | 25 | 28 | 40 | 8 | 1 | 2 | 2 | 1 | 3 | 1 | 1 | 14 | 5 | −0.45 | 13 |
| 26 | 222.0 | 53 | 15 | 2 | 0.301 | 2.0 | 10 | 15 | 21 | 45 | 20 | 6 | 1 | 1 | 2 | 1 | 4 | 1 | 1 | 11 | 6 | −0.26 | 18 |
| 16 | 226.0 | 48 | 6 | 5 | 0.699 | 2.0 | 13 | 10 | 47 | 10 | 50 | 8 | 5 | 4 | 7 | 4 | 5 | 2 | 1 | 28 | 8 | −0.54 | 4 |
| 17 | 227.0 | | 27 | 6 | 0.778 | 4.0 | 20 | 42 | 53 | 14 | 30 | 2 | 3 | 2 | 6 | 3 | 8 | 10 | 6 | 16 | 24 | 0.18 | 16 |
| 19 | 232.0 | | 21 | 9 | 0.954 | 4.0 | 17 | 40 | 55 | 12 | 33 | 1 | 3 | 3 | 5 | 3 | 9 | 7 | 4 | 15 | 20 | 0.12 | 20 |

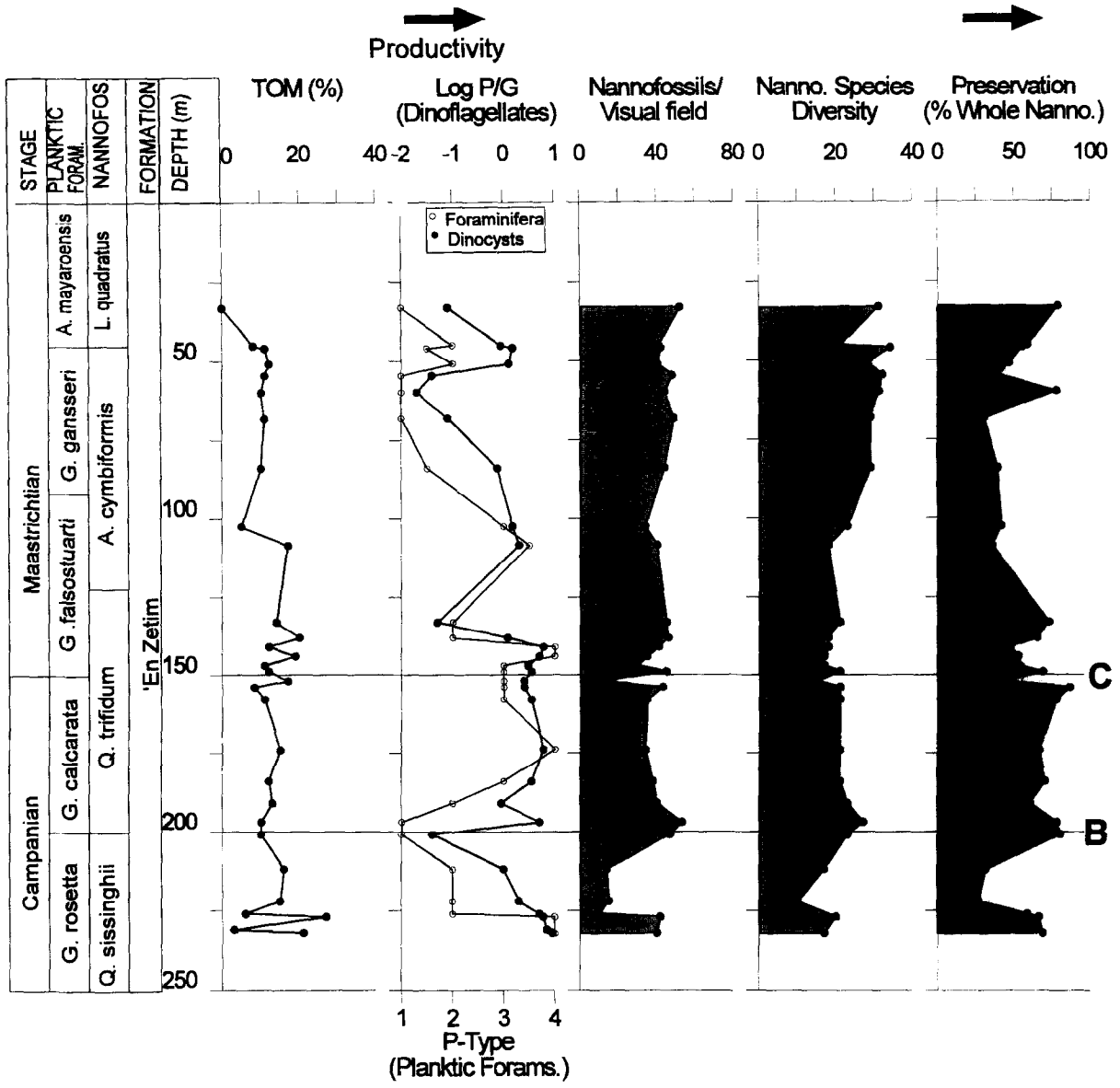


Fig. 2. Total Organic Matter, foraminifera- and dinocyst-based productivity reconstructions, and data on nannofossil assemblages in the Shefela section. For explanation of datum lines, see Fig. 1. Nannofossil zonation after Eshet and Moshkovitz (1995).

and dinocyst productivity reconstructions (Almogi-Labin et al., 1993; Eshet et al., 1994) show nearly identical trends with three clear minima: at the FO of *Quadrum trifidum*, below the last occurrence (LO) of *Q. trifidum* (Early Maastrichtian), and near the FO of *Lithraphidites quadratus*. The interval between the FO of *Q. trifidum* and the base of the Maastrichtian is one of high productivity.

Nannofossil abundance (NVF) shows a general increasing trend from about 30 in the Campanian to more than 40 NVF in the Maastrichtian. It has maxima at the FO of *Q. trifidum* and near the base of the Maastrichtian, and remains uniformly high up to the top of the section. Nannofossil species diversity follows a pattern similar to the nannofossil abundance curve. Nannofossil preservation varies

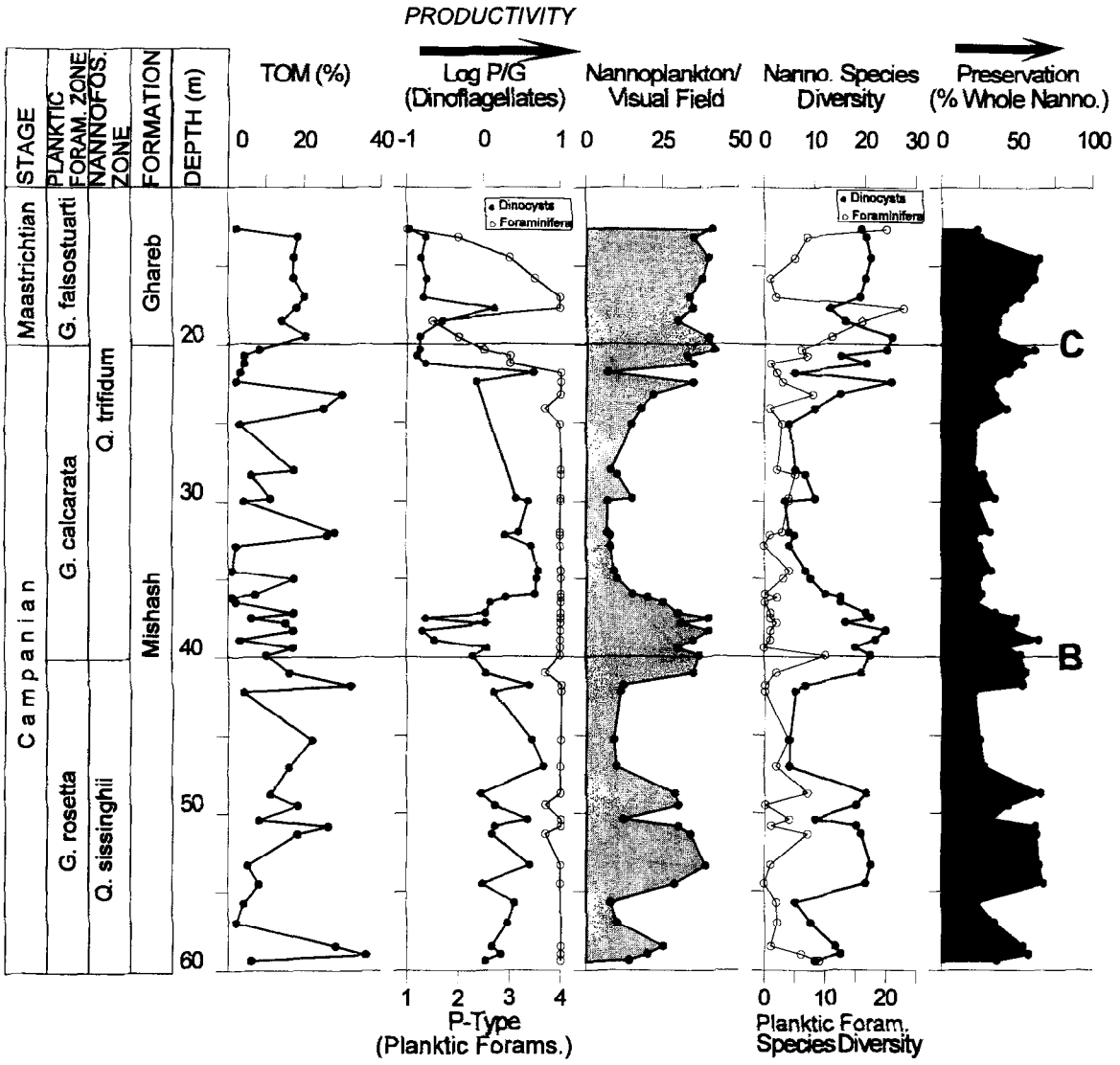


Fig. 3. Total Organic Matter, foraminifera- and dinocyst-base productivity reconstructions, and data on nannofossil assemblages in the Zin section. For explanation of datum lines, see Fig. 1.

throughout the section, with good preservation in the lower part, between the FO of *Q. trifidum* and the base of the Maastrichtian. Highly-dissolved intervals were recognized in the lowermost part of the section and in the *A. cymbiformis* Zone.

**Zin section** (Fig. 3; Table 2): The TOM content in the Zin section is highly variable during the Campanian. A minimum is evident near the Campanian–Maastrichtian boundary, followed by a uniform and high TOM content in the Early Maastrichtian. Dinocyst- and foraminifera-derived productivity indices suggest periods of enhanced productivity during most of the Campanian, except for minima near the FO of *Q. trifidum* (only represented clearly by the dinocyst P/G curve) and at the base of the Maastrichtian. A sharp productivity recovery, followed by a strong decrease, is indicated in the Early Maastrichtian.

Nannofossil abundance (NVF) and species-diversity, as well as planktic foraminifera species-

Table 2
Nannofossil counts in the Zin section. SPC. DIV = Species Diversity; NVF = Nannofossils per Visual Field; PRES. = Preservation; M. DEC. = *Micula decussata*; W. BAR = *W. barnesae*; T. OPER. = *T. operculata*; E. TURR. = *E. turriseiffelii*; PRED. = *Prediscosphaera*; LITHR SPP. = *Lithraphidites* spp.; VEK. & VAG. = *Vekshinella* and *Vagalapilla*; GLAUK. = *Glaukolithus*; BISC. = *Biscutum*; T. SAX. = *Thoracosphaera saxea*. Low PROD. = low productivity; High PROD. = high productivity; NIP = Nannofossil Index of Productivity.

| Sam. no. | Depth m | $CaCO_3$ | TOM % | P-TYPE | P/G | LOG P/G | SPC. DIV | NVF | PRES. % | M. DEC. | W. BAR | T. OPER. | E. TURR. | PRED. SPP | LITHR SPP. | VEK. & VAG. | GLAUK SPP. | BISC. SPP. | T. SAX | Low PROD. | High PROD. | NIP | Others % |
|---|---|---|---|---|---|---|---|---|---|---|---|---|---|---|---|---|---|---|---|---|---|---|---|
| 1 | 12.7 | 63 | 2 | 1 | 0.1 | −1.00 | 19 | 41 | 23 | 40 | 18 | 9 | 4 | 7 | 5 | 2 | 1 | 3 | 0 | 27 | 4 | −0.83 | 11 |
| 2 | 13.2 | 50 | 18 | 2 | 1.2 | 0.08 | 20 | 35 | 25 | 41 | 20 | 7 | 5 | 4 | 5 | 3 | 5 | 7 | 1 | 24 | 13 | −0.27 | 2 |
| 3 | 14.5 | 50 | 17 | 3 | 0.9 | −0.05 | 21 | 40 | 64 | 10 | 20 | 8 | 7 | 5 | 6 | 5 | 3 | 3 | 1 | 31 | 7 | −0.65 | 32 |
| 4 | 15.8 | 59 | 17 | 3.5 | 1.3 | 0.11 | 20 | 38 | 61 | 8 | 18 | 7 | 6 | 5 | 7 | 4 | 4 | 5 | 2 | 29 | 11 | −0.42 | 34 |
| 5 | 17.0 | 56 | 20 | 4 | 1.1 | 0.04 | 19 | 34 | 52 | 20 | 20 | 5 | 5 | 3 | 6 | 3 | 5 | 7 | 3 | 22 | 15 | −0.37 | 23 |
| 6 | 17.7 | 50 | 18 | 4 | 5.7 | 0.76 | 13 | 35 | 42 | 28 | 29 | 5 | 4 | 3 | 5 | 3 | 7 | 6 | 3 | 20 | 16 | −0.10 | 7 |
| 8 | 18.5 | 65 | 14 | 1.5 | 2.3 | 0.36 | 16 | 30 | 37 | 13 | 24 | 6 | 5 | 4 | 7 | 4 | 5 | 4 | 2 | 26 | 11 | −0.37 | 26 |
| 9 | 19.5 | 54 | 20 | 2 | 0.8 | −0.10 | 25 | 40 | 35 | 19 | 29 | 11 | 9 | 9 | 15 | 7 | 1 | 0 | 0 | 51 | 1 | −1.71 | 0 |
| 10 | 20.3 | 53 | 8 | 2.5 | 0.8 | −0.10 | 24 | 42 | 61 | 5 | 26 | 10 | 8 | 7 | 14 | 6 | 1 | 2 | 2 | 45 | 5 | −0.95 | 19 |
| 11 | 20.7 | 46 | 4 | 3 | 0.6 | −0.22 | 15 | 33 | 51 | 10 | 24 | 9 | 4 | 5 | 12 | 3 | 2 | 5 | 4 | 33 | 11 | −0.48 | 22 |
| 12 | 21.2 | 55 | 4 | 3 | 1.2 | 0.08 | 20 | 35 | 53 | 12 | 28 | 8 | 5 | 6 | 12 | 4 | 1 | 4 | 3 | 35 | 8 | −0.64 | 17 |
| 13 | 21.8 | 53 | 3 | 4 | 8.2 | 0.91 | 6 | 7 | 44 | 21 | 26 | 2 | 3 | 2 | 2 | 1 | 12 | 10 | 5 | 10 | 27 | 0.43 | 16 |
| 14 | 22.4 | 67 | 2 | 4 | 4.5 | 0.65 | 25 | 35 | 33 | 28 | 50 | 6 | 5 | 4 | 5 | 3 | 6 | 6 | 3 | 23 | 15 | −0.19 | 4 |
| 15 | 23.2 | 29 | 29.8 | 4 |  | 0.70 | 15 | 22 | 35 | 25 | 29 | 7 | 3 | 6 | 3 | 0 | 5 | 2 | 2 | 19 | 9 | −0.32 | 18 |
| 16 | 24.1 | 26 | 25 | 3.7 |  | 0.80 | 10 | 18 | 43 | 18 | 25 | 5 | 2 | 7 | 2 | 2 | 8 | 6 | 5 | 18 | 19 | 0.02 | 20 |
| 17 | 25.1 | 29 | 3 | 4 |  | 0.85 | 5 | 15 | 1 | 23 | 30 | 3 | 1 | 5 | 1 | 2 | 8 | 7 | 6 | 12 | 21 | 0.24 | 14 |
| 18 | 28 | 20 | 17 | 4 |  | 0.91 | 6 | 8 | 21 | 28 | 35 | 1 | 1 | 4 | 1 | 1 | 10 | 9 | 6 | 8 | 25 | 0.49 | 4 |
| 19 | 28.3 |  | 6 | 4 |  | 0.90 | 8 | 10 | 27 | 28 | 34 | 4 | 2 | 3 | 1 | 0 | 10 | 10 | 5 | 10 | 25 | 0.40 | 3 |
| 20 | 29.8 | 27 | 11 | 4 | 7.1 | 0.85 | 10 | 15 | 35 | 24 | 31 | 5 | 2 | 3 | 2 | 2 | 8 | 9 | 4 | 14 | 21 | 0.18 | 10 |
| 21 | 30.0 | 28 | 4 | 4 | 7.9 | 0.90 | 4 | 7 | 23 | 25 | 38 | 3 | 3 | 0 | 3 | 1 | 10 | 10 | 5 | 10 | 25 | 0.40 | 2 |
| 23 | 32.0 | 44 | 28 | 4 | 7.3 | 0.86 | 5 | 7 | 32 | 22 | 37 | 4 | 3 | 0 | 3 | 1 | 10 | 11 | 5 | 11 | 26 | 0.37 | 4 |
| 22 | 32.2 | 36 | 26 | 4 | 6.4 | 0.81 | 6 | 8 | 22 | 24 | 29 | 5 | 4 | 1 | 1 | 1 | 12 | 9 | 6 | 12 | 27 | 0.35 | 8 |
| 24 | 32.9 | 17 | 2 | 4 | 8.1 | 0.91 | 5 | 8 | 25 | 20 | 24 | 3 | 3 | 1 | 2 | 0 | 11 | 11 | 7 | 9 | 29 | 0.51 | 18 |
| 26 | 34.5 | 81 | 1 | 4 | 8.5 | 0.93 | 8 | 9 | 32 | 25 | 31 | 3 | 4 | 2 | 2 | 2 | 11 | 11 | 9 | 13 | 31 | 0.38 | 0 |
| 27 | 35.0 | 24 | 17 | 4 | 8.4 | 0.92 | 9 | 10 | 24 | 30 | 30 | 4 | 3 | 1 | 1 | 1 | 12 | 10 | 8 | 10 | 30 | 0.48 | 0 |
| 28 | 36.0 | 28 | 7 | 4 | 8.3 | 0.92 | 12 | 15 | 26 | 31 | 28 | 4 | 4 | 2 | 1 | 1 | 10 | 9 | 7 | 12 | 26 | 0.34 | 3 |
| 29 | 36.2 | 79 | 1 | 4 | 6.4 | 0.81 | 15 | 20 | 24 | 32 | 30 | 4 | 5 | 2 | 2 | 2 | 10 | 8 | 5 | 15 | 23 | 0.24 | 0 |
| 30 | 36.5 | 91 | 2 | 4 | 5.4 | 0.73 | 15 | 25 | 22 | 33 | 29 | 5 | 4 | 5 | 3 | 3 | 6 | 6 | 4 | 20 | 16 | −0.02 | 2 |
| 31 | 37.2 | 26 | 17 | 4 | 5.1 | 0.71 | 20 | 30 | 35 | 19 | 27 | 6 | 7 | 8 | 8 | 6 | 8 | 5 | 2 | 35 | 15 | −0.37 | 4 |
| 32 | 37.5 | 14 | 6 | 4 | 1.2 | 0.08 | 21 | 40 | 49 | 17 | 25 | 8 | 7 | 7 | 11 | 5 | 3 | 3 | 2 | 38 | 8 | −0.68 | 12 |
| 33 | 37.8 | 22 | 15 | 4 | 5.1 | 0.71 | 16 | 31 | 48 | 21 | 28 | 5 | 4 | 7 | 6 | 6 | 6 | 8 | 5 | 28 | 19 | −0.17 | 4 |
| 34 | 38.3 | 42 | 17 | 4 | 1 | 0.00 | 24 | 40 | 46 | 20 | 30 | 10 | 7 | 7 | 10 | 6 | 1 | 0 | 3 | 40 | 4 | −1.00 | 6 |
| 35 | 38.9 | 51 | 3 | 4 | 1.8 | 0.26 | 22 | 35 | 64 | 7 | 25 | 8 | 6 | 5 | 8 | 4 | 3 | 5 | 5 | 31 | 13 | −0.38 | 24 |
| 36 | 39.4 | 35 | 17 | 4 | 5.2 | 0.72 | 18 | 30 | 43 | 19 | 32 | 6 | 3 | 6 | 4 | 2 | 6 | 8 | 4 | 21 | 18 | −0.07 | 10 |
| 37 | 39.9 | 25 | 10 | 4 | 4.3 | 0.63 | 21 | 37 | 52 | 8 | 28 | 7 | 5 | 5 | 6 | 3 | 5 | 7 | 2 | 26 | 14 | −0.27 | 24 |
| 38 | 41.0 | 36 | 16 | 3.7 | 5.1 | 0.71 | 19 | 35 | 55 | 10 | 25 | 6 | 4 | 3 | 4 | 3 | 8 | 10 | 4 | 20 | 22 | 0.04 | 23 |
| 40 | 41.8 | 21 | 32 | 4 | 7.9 | 0.90 | 8 | 12 | 53 | 10 | 30 | 4 | 3 | 1 | 1 | 1 | 12 | 12 | 11 | 10 | 35 | 0.54 | 15 |
| 60 | 42.2 | 10 | 4 | 4 | 5.6 | 0.90 | 6 | 11 | 21 | 32 | 29 | 3 | 1 | 1 | 1 | 0 | 13 | 10 | 10 | 6 | 33 | 0.74 | 0 |
| 41 | 45.3 | 29 | 22 | 4 | 8.1 | 0.91 | 5 | 9 | 25 | 34 | 26 | 4 | 2 | 0 | 3 | 1 | 10 | 10 | 9 | 10 | 29 | 0.49 | 1 |
| 42 | 47.0 | 20 | 16 | 4 | 8.9 | 0.95 | 5 | 10 | 28 | 32 | 52 | 3 | 2 | 1 | 3 | 0 | 8 | 8 | 7 | 9 | 23 | 0.56 | 4 |
| 44 | 48.8 | 49 | 11 | 4 | 4.8 | 0.68 | 20 | 29 | 65 | 4 | 50 | 6 | 4 | 2 | 5 | 2 | 8 | 6 | 1 | 19 | 15 | 0.10 | 32 |
| 45 | 49.5 | 50 | 18 | 3.7 | 5.7 | 0.76 | 18 | 30 | 43 | 11 | 28 | 5 | 3 | 1 | 4 | 1 | 10 | 8 | 3 | 14 | 21 | 0.18 | 26 |
| 46 | 50.4 | 13 | 8 | 4 | 7.8 | 0.89 | 10 | 12 | 32 | 8 | 14 | 3 | 2 | 0 | 3 | 0 | 12 | 10 | 5 | 8 | 27 | 0.53 | 43 |
| 47 | 50.8 | 44 | 26 | 4 | 5.7 | 0.76 | 18 | 30 | 61 | 6 | 26 | 5 | 3 | 1 | 4 | 1 | 9 | 8 | 4 | 14 | 21 | 0.18 | 33 |
| 48 | 51.3 | 35 | 18 | 3.7 | 5.5 | 0.74 | 19 | 34 | 62 | 6 | 22 | 4 | 4 | 1 | 3 | 0 | 8 | 7 | 5 | 12 | 20 | 0.22 | 40 |
| 49 | 53.3 | 15 | 5 | 4 | 8 | 0.70 | 21 | 39 | 64 | 9 | 18 | 6 | 3 | 2 | 3 | 1 | 6 | 8 | 4 | 15 | 18 | 0.08 | 40 |
| 51 | 54.5 | 56 | 8 | 4 | 4.9 | 0.69 | 20 | 29 | 67 | 2 | 32 | 4 | 2 | 2 | 3 | 2 | 7 | 8 | 5 | 13 | 20 | 0.19 | 33 |
| 52 | 55.7 | 55 | 4 |  | 7 | 0.85 | 6 | 8 | 23 | 29 | 30 | 1 | 0 | 0 | 1 | 1 | 11 | 10 | 10 | 3 | 31 | 1.01 | 7 |
| 53 | 57 | 52 | 2 |  | 6.5 | 0.81 | 9 | 10 | 34 | 19 | 5 | 1 | 0 | 1 | 1 | 0 | 8 | 8 | 9 | 3 | 25 | 0.92 | 48 |
| 56 | 58.5 | 47 | 28 | 4 | 5.5 | 0.74 | 14 | 25 | 53 | 6 | 6 | 1 | 2 | 1 | 2 | 1 | 7 | 6 | 8 | 7 | 21 | 0.48 | 60 |
| 55 | 59.0 | 42 | 36 | 4 | 6.1 | 0.79 | 15 | 20 | 57 | 10 | 4 | 1 | 1 | 0 | 1 | 1 | 10 | 9 | 9 | 4 | 28 | 0.85 | 54 |
| 57 | 59.4 | 25 | 6 | 4 | 5.1 | 0.71 | 10 | 14 | 36 | 18 | 5 | 2 | 0 | 0 | 1 | 0 | 9 | 8 | 8 | 3 | 25 | 0.92 | 49 |

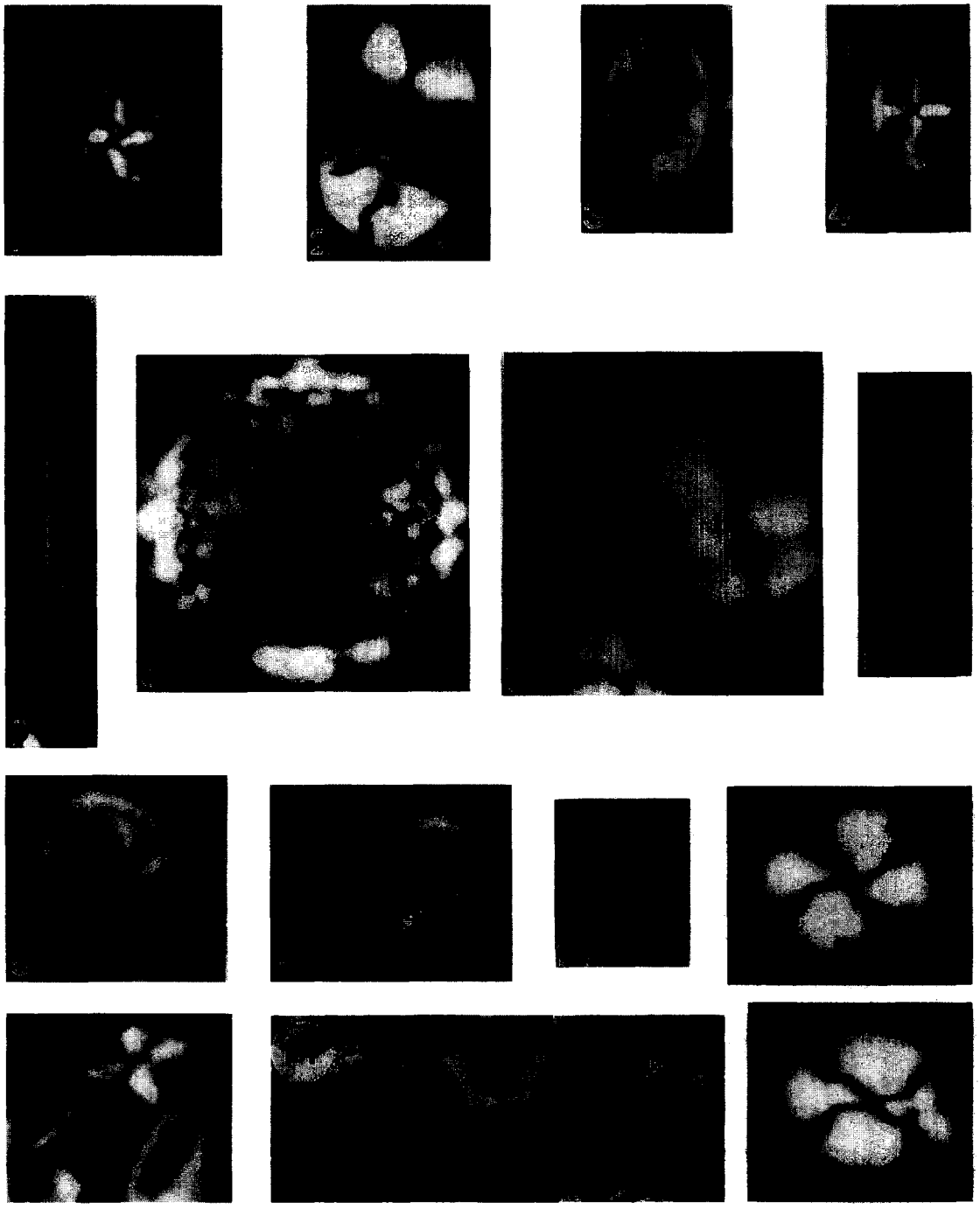

diversity, show similar trends: in general, low abundance and diversity characterize most of the Campanian interval, except for a maximum at the FO of *Q. trifidum*, and at the base of the Maastrichtian. Nannofossil preservation fluctuates throughout the section, with well-preserved intervals near the FO of *Q. trifidum* and in the Early Maastrichtian. The preservation curve shows a very similar pattern as both the abundance and diversity curves.

### 6.2. Distribution of nannofossil taxa

Figs. 4 and 5 show the distribution of the selected prominent taxa in the sections (for the semi-quantitative distribution of all taxa, one is refered to Eshet and Moshkovitz, 1995). In most instances, these taxa comprise more than 80% of the assemblage. Some of the curves represent the combined abundance of all species of one genus (e.g. *Prediscosphaera*, *Lithraphidites*, *Vekshinella*, *Glaukolithus*, *Biscutum*), whereas others represent the distribution of individual species (e.g. *Thoracosphaera operculata*, *Thoracosphaera saxea*, *Eiffellithus turriseiffelii* and *Watznaueria barnesae*). Table 3 lists the species that are included in each of the curves in Figs. 4 and 5. *Vekshinella* and *Vagalapilla* were combined in one curve due to the difficulties in distinguishing between the two genera.

The distribution patterns of the selected nannofossils enabled the establishment of three distinct groups of taxa. These groups are labeled I–III in Figs. 4 and 5, and their members are listed in Table 3.

The curves indicate the following trends:

**Shefela section** (Fig. 4): *T. operculata*, *Eiffellithus* spp., *Prediscosphaera* spp., *Lithraphidites* spp. and *Vekshinella* spp. (Group I) attain maximum abundance at the FO of *Q. trifidum* (Datum B) and minimum abundance at the base of the Maastrichtian (Datum C), with a slightly increasing trend above this datum. *Glaukolithus* spp., *Biscutum* spp. and *Thoracosphaera saxea* (Group II) show an opposite pattern of distribution compared to Group I. *Micula decussata* is prominent in most samples, with peaks in the lower part of the section and in the Maastrichtian (*A. cymbiformis* Zone - NC 21). *Watznaueria barnesae* is the most abundant taxon, with high abundance during most of the Campanian, and a slight decrease during the Early Maastrichtian.

**Zin section** (Fig. 5): Species belonging to Group I have two clear maxima: near the FO of *Q. trifidum* and at the base of the Maastrichtian. Members of Group II show an opposite trend of abundance compared to Group I. *Micula decussata* and *W. barnesae* (Group III) are the dominant taxa in the section, with a nearly-uniform pattern of distribution for *Watznaueria*, whereas *Micula*'s abundance changes are more pronounced.

Some consistent relationships between the groups can be inferred by comparing their distribution in both sections (Figs. 4 and 5): Groups I and II show

---

Plate I

Representative nannofossils of Groups I–III. All light microscope photographs are ×3750.

**Group I**

1. *Prediscosphaera spinosa.* Shefela Basin, sample ZRB 25.
2. *Eiffellithus turriseiffelii.* Shefela Basin, sample HRB 29.
3. *Eiffellithus gorkae.* Zin Basin, sample SA 24.
4. *Vekshinella stradneri.* Shefela Basin, sample ZRB 12.
5. *Lithraphidites carniolensis.* Shefela Basin, sample ZRB 12.
6. *Thoracosphaera operculata.* Shefela Basin, sample ZRB 25.

**Group II**

7. *Thoracosphaera saxea.* Shefela Basin, sample ZRB 8.
8. *Lithraphidites quadratus.* Shefela Basin, sample ZRB 3.
9. *Glaukolithus diplogrammus.* Zin Basin, sample SA 33.
10. *Zygodiscus spiralis.* Shefela Basin, sample ZRB 5.
11. *Biscutum constans.* Shefela Basin, sample ZRB 13.

**Group III**

12, 15. *Watznaueria barnesae.* Zin Basin, sample SA 3.
13. *Micula decussata.* Shefela Basin, sample ZRB 9.
14. *Micula decussata* ooze. Shefela Basin, sample HRB 26.

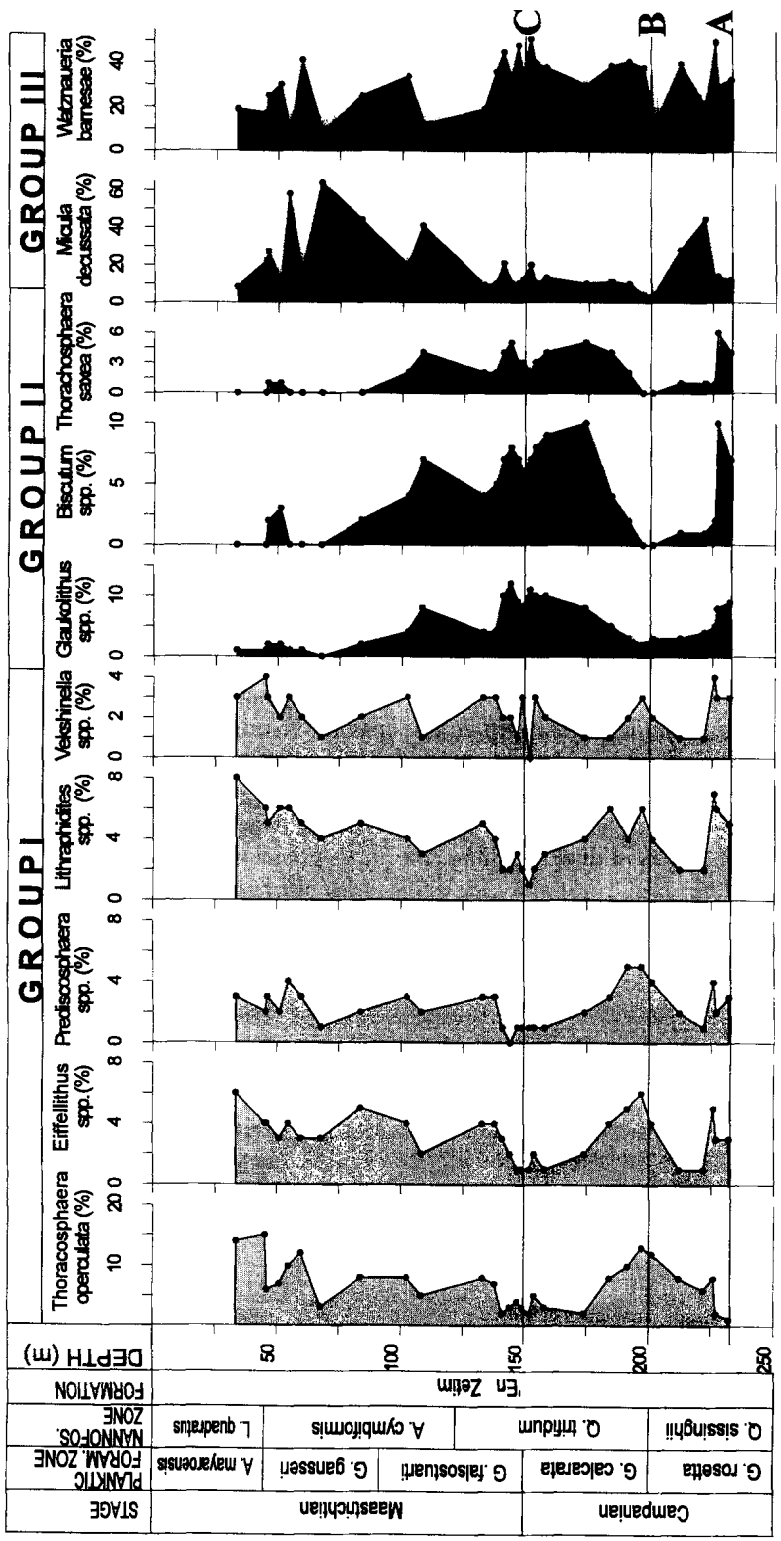


Fig. 4. Abundance distribution and grouping of selected nannofossil taxa in the Shefela section.

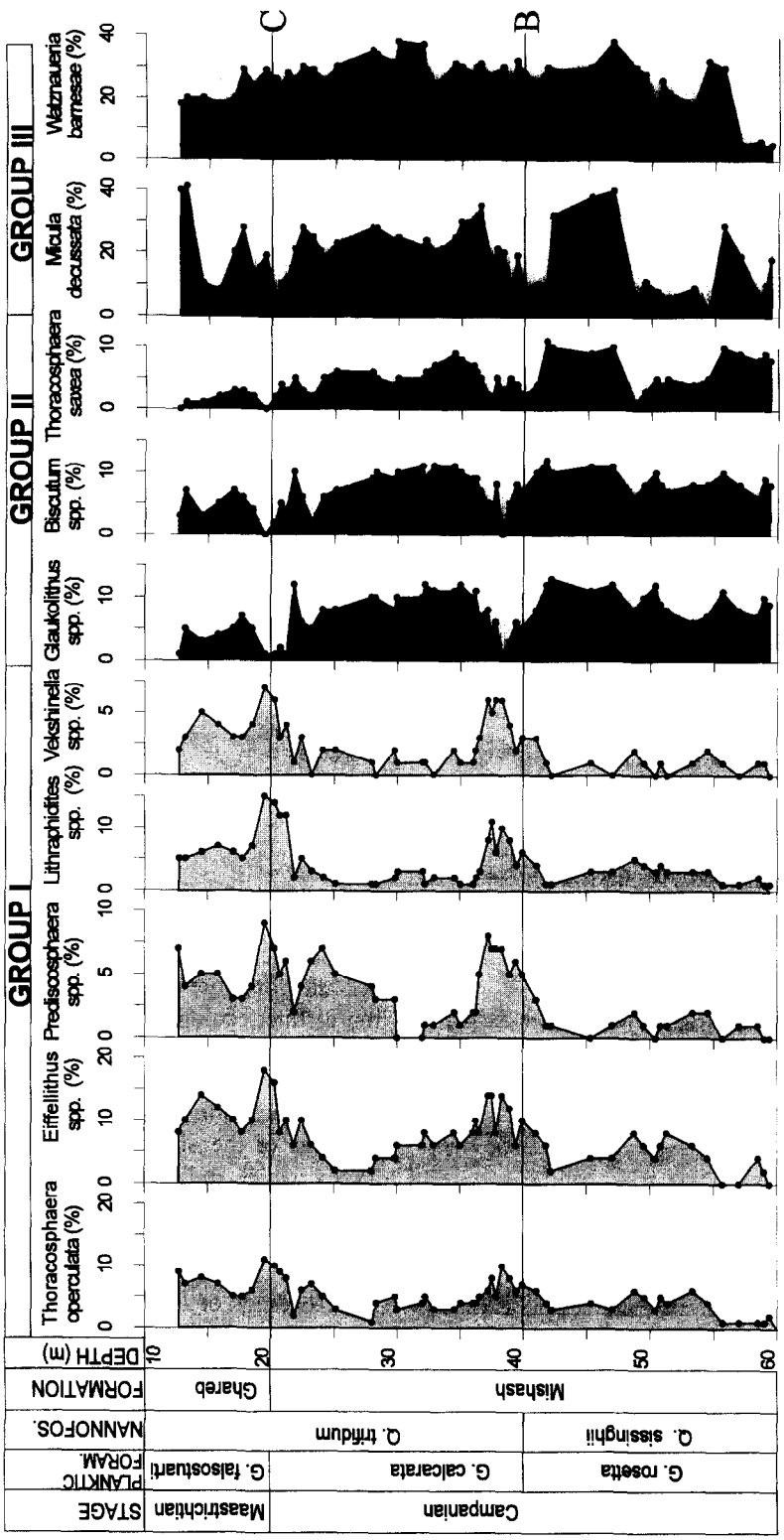


Fig. 5. Abundance distribution and grouping of selected nannofossil taxa in the Zin section.

Table 3
Nannofossil taxa included in Groups I–III. For taxa distribution, see Figs. 4, 5. Selected species are illustrated in Plate I. Taxa in bold letters represent the curve-title in Figs. 4 and 5.

**Group I**
***Eiffellithus* spp.**
*Eiffellithus eximius* (Stover, 1966) Perch-Nielsen, 1968
*Eiffellithus gorkae* Reinhardt, 1965
*Eiffellithus parallelus* Perch-Nielsen, 1973
*Eiffellithus turriseiffelii* (in Deflandre and Fert, 1954) Reinhardt, 1965

***Lithraphidites* spp.**
*Lithraphidites carniolensis* Deflandre, 1963
*Lithraphidites praequadratus* Roth, 1978
*Lithraphidites quadratus* Bramlette and Martini, 1964
*Microrhabdulus decoratus* Deflandre, 1959

***Prediscosphaera* spp.**
*Prediscosphaera cretacea* (Arkhangelsky, 1912) Gartner, 1968
*Prediscosphaera quadripunctata* (Gorka, 1957) Reinhardt, 1970
*Prediscosphaera spinosa* (Bramlette and Martini, 1964) Gartner, 1968

***Thoracosphaera operculata***
*Thoracosphaera operculata* Bramlette and Martini, 1964

***Vekshinella* spp.**
*Vagalapilla imbricata* (Gartner, 1968) Bukry, 1969
*Vagalapilla matalosa* (Stover, 1966) Thierstein, 1973
*Vekshinella stradneri* Rood et al., 1971

**Group II**
***Glaukolithus* spp.**
*Glaukolithus compactus* (Bukry, 1967) Perch-Nielsen, 1984
*Glaukolithus diplogammus* (Deflandre in Deflandre and Fert, 1954) Reinhardt, 1964
*Zygodiscus spiralis* Bramlette and Martini, 1966

***Biscutum* sp.**
*Biscutum constans* (Gorka, 1957) Black in Black and Barnes, 1959

***Thoracosphaera saxea***
*Thoracosphaera saxea* Stradner, 1961

**Group III**
***Micula* sp.**
*Micula decussata* Vekshina, 1959

***Watznaueria* sp.**
*Watznaueria barnesae* (Black in Black and Barnes, 1959) Perch-Nielsen, 1968

mirror-image abundance profiles. This pattern seems to prevail throughout the entire succession in both sections, even in poorly-preserved samples. Distribution patterns for Group III are more complex and are discussed in the 'Nannofossil Preservation and Productivity' section below.

Table 4
Loadings of the different variables on the four principal components in the Shefela Basin

| Variable | 1 | 2 | 3 | 4 |
|---|---|---|---|---|
| $CaCO_3$ | 0.22 | **0.57** | 0.28 | −0.006 |
| TOM | **0.63** | −0.32 | 0.02 | −0.12 |
| Log P/G | **0.75** | −0.003 | −0.47 | 0.03 |
| P-Type | **0.91** | 0.07 | −0.14 | −0.24 |
| Spec. Div. | −0.44 | 0.001 | **0.60** | 0.32 |
| NVF | −0.06 | 0.23 | **0.82** | 0.34 |
| Preservation | 0.11 | **0.86** | 0.15 | 0.27 |
| *M. decussata* | −0.24 | **−0.87** | 0.26 | −0.17 |
| *W. barnesae* | 0.31 | 0.32 | **−0.77** | −0.05 |
| *T. operculata* | **−0.78** | 0.26 | 0.04 | 0.44 |
| *E. turriseiffelii* | −0.34 | 0.13 | 0.16 | **0.83** |
| *Prediscosphaera* spp. | −0.36 | 0.12 | −0.05 | **0.77** |
| *Lithraphidites* spp. | −0.25 | 0.09 | 0.22 | **0.82** |
| *Veksinel.&Vagalapil.* | −0.02 | 0.28 | 0.13 | **0.68** |
| *Glaukolithus* spp. | **0.80** | 0.19 | −0.24 | −0.42 |
| *Biscutum* spp. | **0.90** | 0.17 | −0.03 | −0.31 |
| *T. saxea* | **0.93** | 0.13 | −0.001 | −0.19 |
| Group I | **−0.57** | 0.21 | 0.09 | **0.76** |
| Group II | **0.90** | 0.18 | −0.11 | −0.34 |
| NIP (log Groups II/I) | **0.78** | −0.02 | −0.19 | **−0.54** |
| Others | −0.27 | **0.55** | 0.47 | 0.001 |
| Total variance explained | 48.10 | 16.64 | 8.65 | 6.41 |
| Cummulative % | 48.10 | 64.75 | 73.40 | 79.81 |

Significant values in bold.

### 6.3. Statistical analysis

Four factors were determined for each basin. They account for more than 80% of the variance, showing distinct ecological patterns. The loadings of the different variables on these four factors are listed in Tables 4 and 5.

**Shefela Basin** (Table 4): Factor 1 comprises high loadings of the absolute values of log P/G and P-Types, which indicates that it represents productivity. This factor is also characterized by high loadings of species of Group II, namely *Glaukolithus* spp., *Biscutum* spp. and *T. saxea*. Factor 2 comprises high loadings of the variables Preservation, $CaCO_3$ content and *M. decussata*, which suggests that it represents preservation. Factor 3 is characterized by high loadings of the variables Species Diversity and Nannofossil per Visual Field (NVF), which may indicate that in the Shefela Basin, this factor represents favorable marine environments for the development of calcareous nannoplankton. Factor 4 is character-

Table 5
Loadings of the different variables on the first four principal components in the Zin Basin

| Variable | 1 | 2 | 3 | 4 |
|---|---|---|---|---|
| $CaCO_3$ | 0.24 | −0.03 | −0.12 | **−0.68** |
| TOM | −0.05 | 0.14 | −0.17 | **0.76** |
| Log P/G | **−0.79** | 0.07 | 0.45 | 0.15 |
| P-Type | **−0.57** | 0.31 | **0.54** | 0.14 |
| Spec. Div. | **0.74** | 0.44 | −0.09 | −0.20 |
| NVF | **0.79** | 0.38 | −0.18 | −0.16 |
| Preservation | 0.26 | **0.89** | −0.04 | 0.06 |
| *M. decussata* | −0.10 | **−0.90** | 0.01 | −0.13 |
| *W. barnesae* | 0.10 | −0.32 | **0.82** | −0.12 |
| *T. operculata* | **0.92** | −0.02 | 0.04 | −0.07 |
| *E. turriseiffelii* | **0.86** | 0.005 | 0.21 | −0.06 |
| *Prediscosphaera* spp. | **0.89** | −0.06 | −0.09 | 0.09 |
| *Lithraphidites* spp. | **0.89** | 0.11 | 0.05 | 0.003 |
| *Veksinel. & Vagalapil.* | **0.88** | 0.05 | 0.18 | 0.02 |
| *Glaukolithus* spp. | **−0.87** | −0.14 | 0.21 | 0.17 |
| *Biscutum* spp. | **−0.87** | −0.10 | 0.20 | 0.12 |
| *T. saxea* | **−0.76** | −0.08 | 0.07 | 0.28 |
| Group I | **0.96** | 0.03 | 0.11 | −0.04 |
| Group II | **−0.91** | −0.11 | 0.18 | 0.20 |
| NIP (log Groups II/I) | **−0.96** | 0.0004 | −0.02 | 0.11 |
| Others | −0.19 | **0.77** | **−0.55** | 0.06 |
| Total variance explained | 55.69 | 14.17 | 6.92 | 4.56 |
| Cummulative % | 55.69 | 69.86 | 76.78 | 81.34 |

Significant values in bold.

ized by high loadings of taxa from Group I, namely *E. turriseiffelii*, *Prediscosphaers* spp., *Lithraphidites* spp., *Veksinella* spp. and *Vagalapilla* spp. It is suggested that factor 4 represents intervals of lower productivity based on the interpretation of Group I as indicator of lower productivity (see discussion below).

**Zin Basin** (Table 5): Factors 1 and 2 are very similar in their variance and high loadings to the Shefela Basin. Factor 1 also comprises high loadings of species diversity and abundance (NVF), which are reciprocal to the productivity-indicators P/G and P-Types. Factor 3 comprises high loadings of P-Types and *W. barnesae*, reflecting probable relationships between this known solution-resistant taxon and productivity. Factor 4 comprises high reciprocal loadings of $CaCO_3$ and TOM, suggesting a negative correlation between carbonate precipitation and organic matter accumulation and preservation.

To conclude, strong loadings on productivity indicators in both basins explain 50–55% of the variance. Preservation indicators explain 15%.

## 7. Discussion

### 7.1. Nannofossil populations

The relationship between calcareous nannoplankton and productivity was discussed in various studies of both the living and fossil record. Jimenez (1981) observed that the nannoplankton population increases from the center of the Galapagos upwelling system towards its margins. Ziveri et al. (1995) reported that maximum coccolithophore flux in the southern California upwelling system (San Pedro Basin) correlates with "peak stratification of the upper water column, low total primary production, and low nutrient content." Thunell and Sautter (1992) reported on inverse population relationships between nannoplankton and foraminifera, suggesting that during peaks of productivity, the nannoplankton population declines whilst the proportion of foraminifera in the sediment increases. Young (1994) indicated that in normal marine conditions, the nannoplankton population increases with productivity, but that in extreme eutrophic environments, the population is suppressed and decreases significantly. In many studies (e.g. Reid et al., 1978), diatoms and organic-walled heterotrophic dinoflagellates are found as the dominant plankton in upwelling areas, whereas in gyre-centers and low-productivity areas, calcareous nannoplankton becomes the dominant phytoplankton (Reid, 1980).

Looking at the fossil record, in a paleoceanographic study of the Greenhorn Formation, Watkins (1989) reported that nannofossil assemblages showed increase in abundance and diversity in intervals that were deposited under low productivity conditions, whereas in intervals that represent enhanced productivity, the nannofossil assemblages were impoverished. Blooms of nannoplankton in conditions of low productivity were also described from K/T boundary layers in Israel (Eshet et al., 1992).

Results of the present study (Figs. 2 and 3) indicate that nannofossils reach their highest species diversity and abundance in intervals of lowered productivity. Conversely, abundance and diversity decline in intervals of the heightened productivity, where the nannoplankton populations are suppressed by the extreme

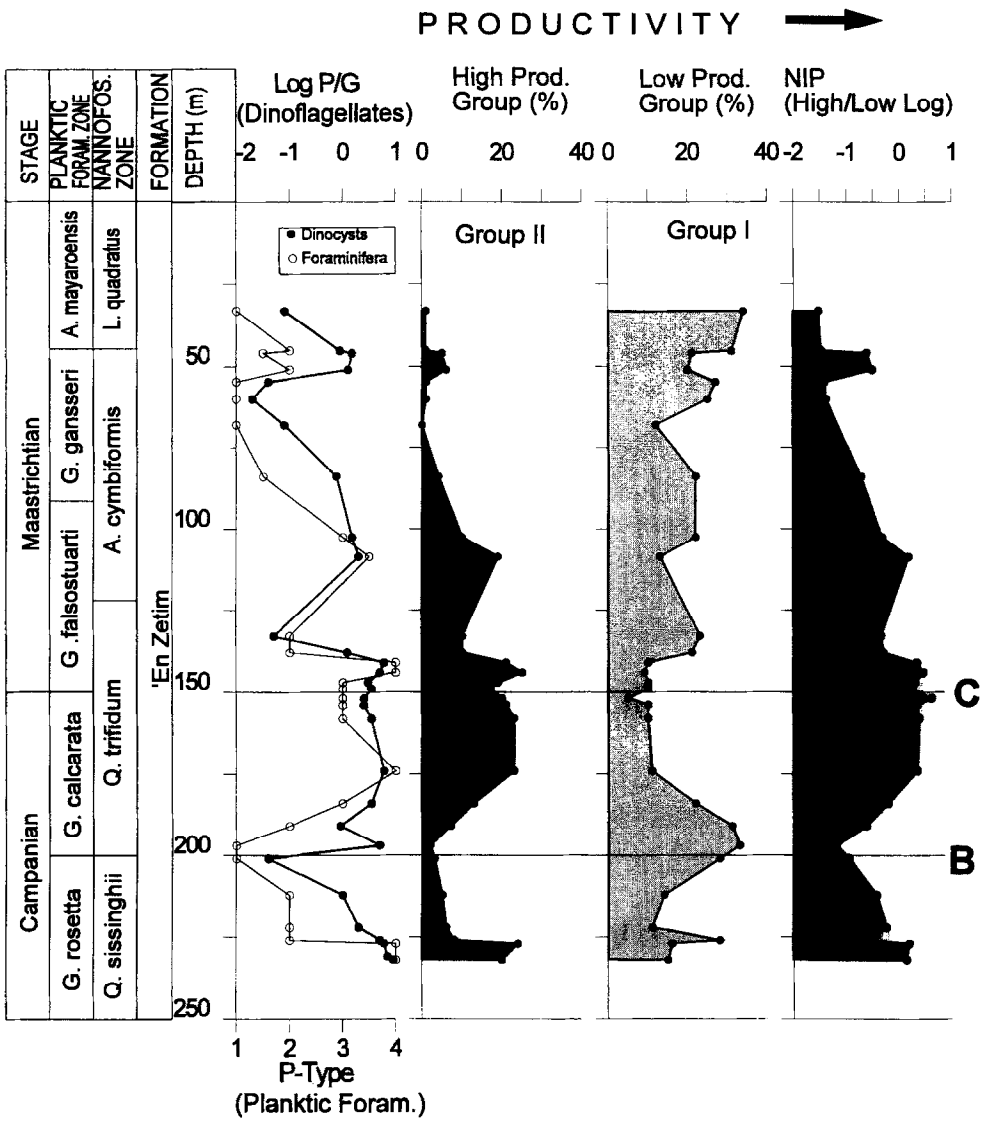


Fig. 6. The Nannofossil Index of Productivity and its comparison to planktic foraminifera- and dinocyst-based productivity reconstructions in the Shefela section. Note excellent match between NIP, P/G and P-Type curves.

productivity conditions. The relationships between productivity and the nannoplankton population are illustrated by the high reciprocal loadings of Species Diversity and Nannofossils per Visual Field (NVF) on Factor 1 in the Zin Basin (Table 5).

### 7.2. *Nannofossil groups and productivity*

As in most upwelling systems, change in nutrient flux is the major factor that affects the distribution of plankton. Correlation of the curves of nannofossil Groups I–II (Figs. 4 and 5) with the dinocyst- and foraminifera-based productivity curves (Figs. 2 and 3), as well as their high loadings on Factor 1 (Tables 4 and 5) indicates that Group I shows increase in intervals of decreasing productivity, whereas, in intervals of increasing productivity, Group II increases (Fig. 6).

The identification of specific nannofossil taxa as indicators of productivity in literature is very lim-

ited. Despite this fact, similar conclusions have been arrived at in several studies, concerning the significance of taxa from groups I and II. Watkins (1989), suggested that intervals of low productivity are characterized by a higher abundance of, among others, *Vekshinella stradneri*, *Prediscosphaera spinosa* and *Lithraphidites carniolensis*, all of which are typical of Group I. Other taxa that Watkins (1989) classified as indicators of lower productivity are *Tranolithus orionatus* and *Zygodiscus theta*, which occur in very low numbers in our samples. Watkins (1989), Roth (1981), Roth and Bowdler (1981), Roth and Krumbach (1986) and Erba et al. (1992) also suggested that *Zygodiscus erectus* and *Biscutum constans*, members of Group II, represent intervals of higher productivity. In the present study, we found that the distribution of *Glaukolithus* spp. (possible paleoenvironmental equivalents of *Z. erectus*), and *Thoracosphaera saxea* can also be used as indicators of high productivity. The calcareous dinoflagellate cyst *T. operculata* (Fütterer, 1976) is included in Group I based on the study of Eshet et al. (1992) that suggested its significance as an indicator of low productivity. Lamolda et al. (1992) and Erba et al. (1992) referred to *W. barnesae* as an indicator of low productivity, but commented that the occurrence of this solubility-resistant taxon is also affected by preservation, as proposed by Roth and Krumbach (1986). Based on these arguments, we suggest that the distribution of nannofossils from Groups I and II can be used as a sensitive proxy of paleoproductivity in upwelling, or other high productivity conditions. This is clearly indicated by the high absolute loadings of Groups I and II and their associated taxa, on Factor I in both Basins (Tables 4 and 5). Of course, these groups may require modification in different oceanic environments, where different ecological conditions may create different productivity signals.

### *7.3. Towards establishing nannofossils as indicators of productivity: the NIP Ratio*

The good correlation between the distribution of nannofossils (Figs. 2 and 3) and the foraminifera- and dinocyst-derived paleoproductivity profiles allow the characterization of high and low productivity conditions (Figs. 4 and 5).

- **Low productivity**: Assemblage characterized by high nannofossil abundance and species diversity. It includes taxa from Group I: *T. operculata*, *Eiffellithus* spp. (mainly *E. turriseiffelii*), *Prediscosphaera* spp. (mainly *P. cretacea* and *P. spinosa*), *Lithraphidites* spp. (mainly *L. carniolensis*), as well as *Vekshinella* and *Vagalapilla*. These taxa have high absolute loadings on Factor 1, and in the Shefela Basin also on Factor 4 (Tables 4 and 5).
- **High productivity**: Assemblage characterized by a lower nannofossil abundance and species diversity. It includes taxa from Group II: *Glaukolithus* spp., *Biscutum* spp. and *T. saxea*, which have high absolute loadings on Factor 1.

Given these relationships, we propose the Nannofossil Index of Productivity (NIP) as a sensitive proxy of productivity. This index is the logarithmical value of the ratio between Group II (high productivity) and Group I (lower productivity):

$$\text{NIP} = \text{Group II}/\text{Group I}(\log)$$

A logarithmic scale is used to construct the NIP curve because it enables consistent recording of shifts in productivity at both high and low productivities. The logarithmic scale was used similarly by Powell et al. (1990), Lewis et al. (1990) and Eshet et al. (1994) to construct the P/G (1994) curve as a paleoproductivity proxy.

The sensitivity of the NIP to productivity changes, and its utility as a paleoproductivity proxy, is illustrated by the good correlation between the NIP and the dinocyst- (P/G) and foraminifer- (P-Types) based productivity profiles (Figs. 6 and 7), and by the high absolute loadings of NIP on Factor 1. In most samples, Group III comprises the majority of the assemblage and Groups I and II are relatively small (Tables 1 and 2). This suggests that the clear reciprocal relationships between Groups II and I are genuine and not an artificial ratio between two very large groups that comprise the bulk of the assemblage.

### *7.4. Nannofossil Index of Productivity and tracing productivity history*

The utility of the NIP in reconstructing the spatial and temporal development of productivity in the study area is illustrated in Fig. 8, where it is plotted against

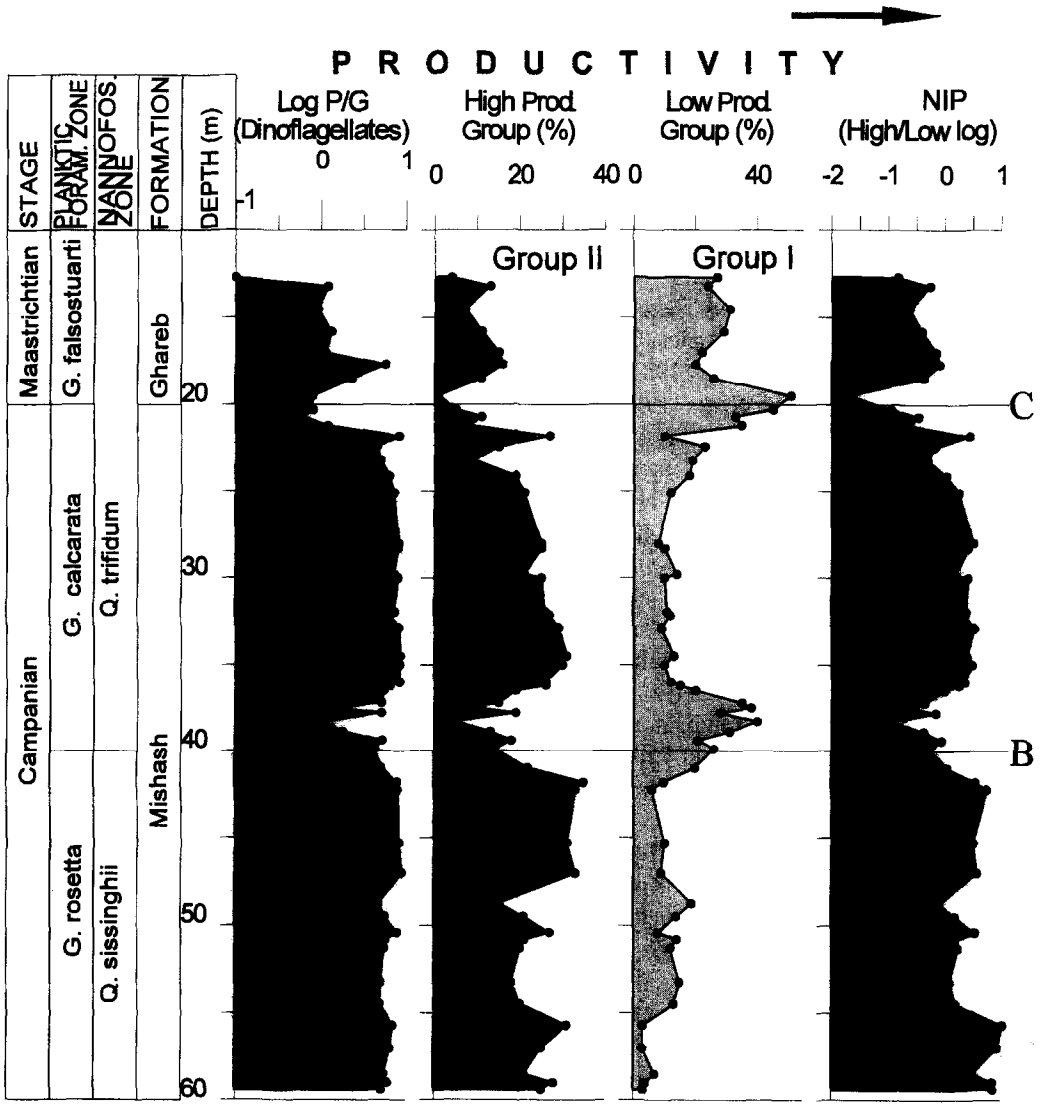


Fig. 7. The Nannofossil Index of Productivity and its comparison to dinocyst-based productivity reconstructions in the Zin section. Note excellent match between NIP and P/G curves.

the other available productivity proxies. The P-Type curve of the Zin Basin is not included since, due to the low abundance of foraminifera in this section, it does not provide useful data (see Fig. 3). Since the NIP is sensitive to productivity changes in both basins, it can be utilized to obtain a more detailed comprehensive understanding of the productivity history of the basins (Fig. 8). Comparison of the NIP curves in the two sections suggests that during the Late Campanian, productivity was high in both basins. A trend of decreasing productivity is seen in both basins in the Late Campanian, culminating in a productivity minimum at the FO of *Q. trifidum*. This minimum was probably very strong because it is reflected in the distribution of all the productivity-significant nannofossil groups (Figs. 4 and 5).

The NIP curve (Fig. 8) indicates that in both basins, the productivity minimum near the FO of *Q. trifidum* was followed by a cycle that began with a sharp rise in productivity and ended in

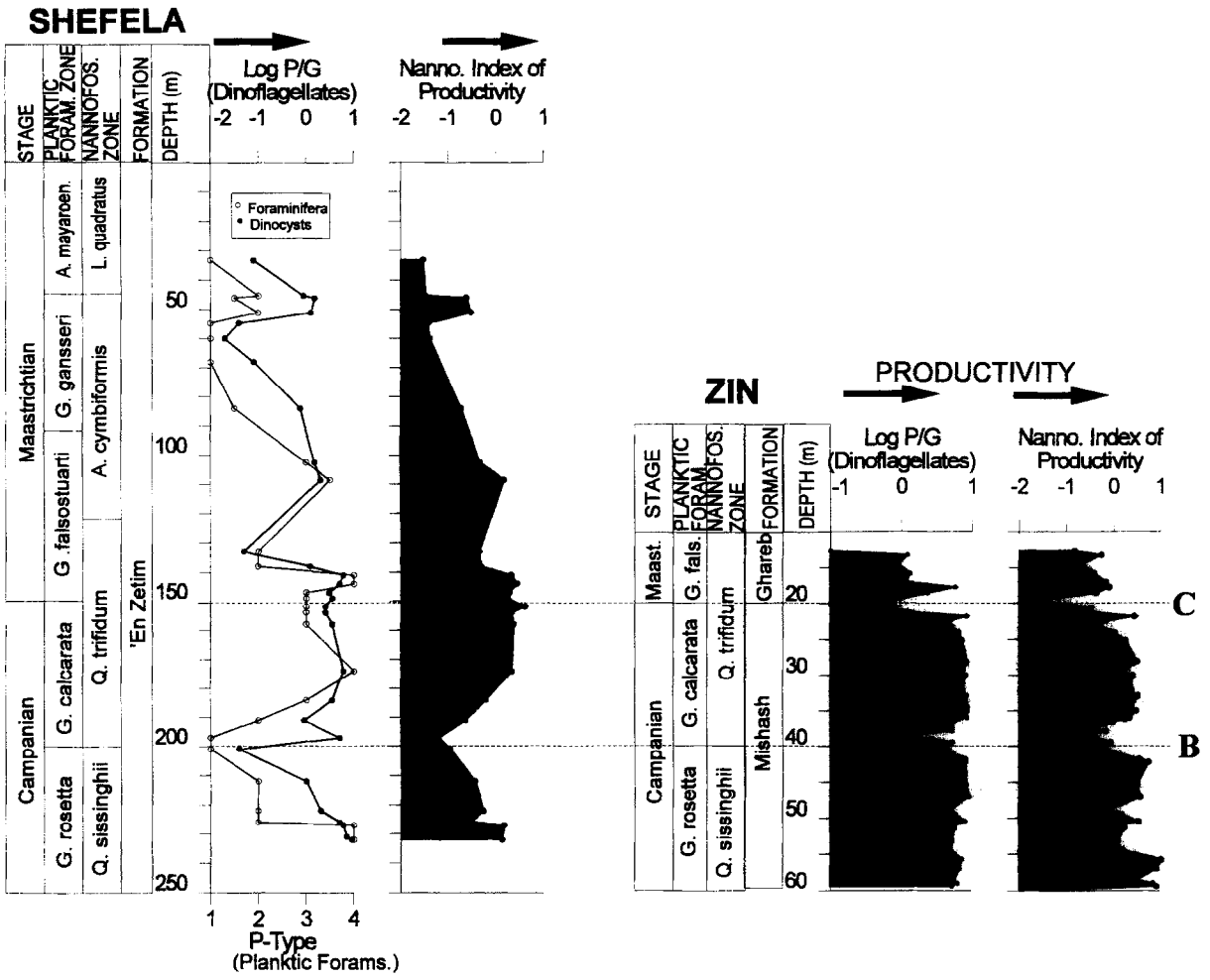


Fig. 8. Correlation of the Nannofossil Index of Productivity between the Zin and Shefela sections, with comparison to foraminifera- and dinocyst-based productivity profiles.

a productivity minimum toward the Campanian–Maastrichtian boundary (Datum C). This minimum, which is well-manifested by the dinocysts (P/G ratio) and foraminifera (P-Types), was diachronous: it occurred first in the Zin Basin, near the Campanian–Maastrichtian boundary, and later in the Shefela Basin. In the Early Maastrichtian, the NIP, the P/G ratio and P-Types in both basins indicate the occurrence of another productivity cycle that began with a productivity rise at the top of the *Quadrum trifidum* Zone, and ended with a productivity minimum in the *Arkhangelskiella cymbiformis* Zone.

### 7.5. Paleogeographic implications

Analysis of nannofossil assemblage composition, combined with data from foraminifera and dinoflagellates, can be used to test previously-published paleogeographic models for the Campanian–Maastrichtian in Israel (e.g. Gvirtzman et al., 1989). Almogi-Labin et al. (1993) suggested that during Campanian–Maastrichtian times, central and northwestern Israel were located on the upper slope, in the marginal, seaward side of the upwelling system, whereas inner shelf basins (represented by the Zin Basin) existed in southern Israel). According to them, a thin layer of well-aerated surface wa-

ter existed in the Zin Basin, overlying the Oxygen Minimum Zone (OMZ), which extended from very close to the water surface to the sea-floor during times of maximum productivity. Conversely, in the Shefela Basin, the OMZ never did reach the sea-floor. These results suggest that a transect from the Zin to the Shefela Basins can be regarded as a line crossing the upwelling belt from its center (Zin) to its margin (Shefela). Similar observations were made by Eshet et al. (1994), who found that peridinioid dinocysts, which are considered representatives of heterotrophic (non-photosynthetic) phytoplankton, are more dominant in the Zin than in the Shefela Basin. In the present study, the nannofossil assemblages (Figs. 2 and 3) indicate that species diversity and abundance are significantly higher (and the corresponding NIP values are significantly lower) on the seaward side of the upwelling system (Shefela), compared to the central, more productive part (Zin). This observation probably reflects the suppression of the nannoplankton populations in extreme productivity conditions (Young, 1994). The more favorable conditions for the development of nannoplankton in the Shefela Basin are reflected by the high loadings of Nannofossil per Visual Field and Species Diversity on Factor 3 (Table 4), compared to the low loadings in the Zin Basin (Table 5).

### 7.6. Nannofossil preservation and productivity

Calcareous nannofossils are subject to various processes of preservation or destruction in the sea bottom. Schlanger et al. (1973), Roth and Berger (1975) and Matter et al. (1975) made observations on the dissolution of calcareous nannofossils in marine sediments. Roth (1994) described the distribution and preservation of calcareous nannofossils in sediment in different oceanic environments. The relationship between nannofossil preservation and OM accumulation was examined by Roth (1983) and Roth and Krumbach (1986), who showed the existence of an inverse relationship between TOM and total coccolith abundance in the sediment.

Rocks in the studied sections were deposited well above the CCD, and therefore, their preservation is mainly a function of the interplay between the rate of OM accumulation (= productivity), oxygen content at the bottom, and diagenesis.

Hill (1975) and Thierstein (1980) have experimentally investigated the solubility resistance of Late Cretaceous nannofossil taxa. They found that the smallest nannofossils, and those with fine structures, are the most solution-susceptible. Thierstein (1980) discovered that most taxa did not show a significant abundance change with dissolution, and only two small groups, of solution-resistant and solution-susceptible taxa, could be discerned. Among his most solution-resistant taxa, which are common to abundant in the present study, are *Micula (staurophora)* (= *M. decussata*), *Thoracosphaera operculata* and *Watznaueria barnesae*. From Thierstein's most solution-susceptible taxa we note here *Biscutum (constans)*, *Prediscosphaera (spinosa)* and *Cribrosphaerella ehrenbergii*.

Based on the solutionability-resistance of *W. barnesae*, Roth and Krumbach (1986) and Lamolda et al. (1992) suggested that positive correlations between the distribution of *W. barnesae* and TOC indicate that most of the nannofossil dissolution resulted from the release of carbon dioxide from oxidized OM. They also noted a positive correlation between nannofossil species diversity and assemblage preservation.

The foraminiferal assemblages in the studied sections (Almogi-Labin et al., 1993) point to changing modes of prevailing sea-floor processes during the studied time-interval: in the Shefela Basin, preservation was affected mainly by dissolution, whereas in the Zin section, precipitation of sparry calcite was dominant. Since dissolution and spar precipitation, both produce incomplete fossils, it was not possible to distinguish between the two processes in the present study.

Comparison of nannofossil preservation with the OM content, productivity profiles, and nannofossil abundance and diversity (Figs. 2 and 3) shows that, despite the fact that in general intervals with high OM content are associated with poor preservation, there are intervals that show the opposite, and no clear preservation – OM content relationship is evident. This is illustrated by the low loadings of TOM on Factor 2.

In the studied sections, delicate and solution-susceptible taxa (e.g. *B. constans*, *P. cretacea*, *P. spinosa*, *Nephrolithus frequens*) are fairly common and well-preserved. This may suggest that the effect of dissolution on assemblage composition is lim-

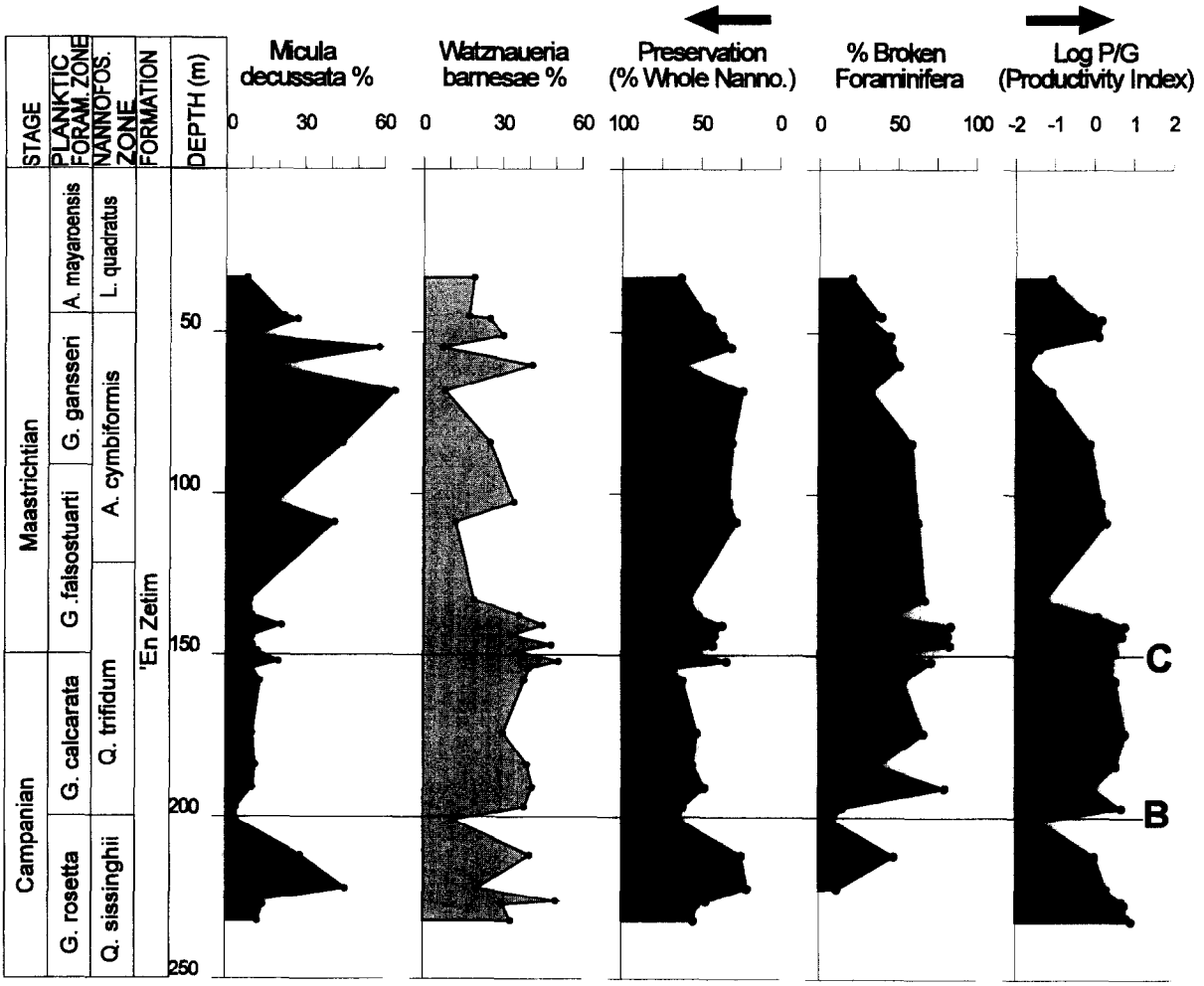


Fig. 9. Shefela section: Nannofossil preservation and the distribution of *M. decussata* and *W. barnesae*, compared to preservation of foraminifera.

ited, and that dissolution did not eliminate species completely from the assemblage. This conclusion is supported by the good match between nannofossil species diversity and the productivity curves in Figs. 2 and 3. Dissolution does seem to have an effect on nannofossil abundance, which tends to decrease in poorly-preserved samples.

In the studied basins, *Micula* and *Watznaueria*, two of the most solution-resistant taxa of Hill (1975), Thierstein (1980) and Roth and Krumbach (1986), usually predominate in the assemblages. Our results indicate that *W. barnesae* is not only a 'preservation indicator'. In intermediate levels its distribution is strongly affected by productivity. The distribution pattern of *W. barnesae* correlates generally with the productivity curves in intermediate productivity levels (Shefela section, Fig. 9), and with Factor 3 in the Zin section (Table 5).

Figs. 9 and 10, and the high negative loadings on Factor 2, show that *Micula* has a negative correlation with preservation: it becomes more common in poorly-preserved samples, and usually reaches its lowest occurrence in well-preserved ones. In particularly poorly-preserved intervals, *Micula* becomes extremely dominant and forms a '*Micula* ooze'. This observation supports the determination of *Micula* as a solution-resistant taxon (Thierstein, 1980) and suggests its utility as an indicator of sea-floor processes and diagenesis. A similar pattern, although less pronounced, is observable in the preservation

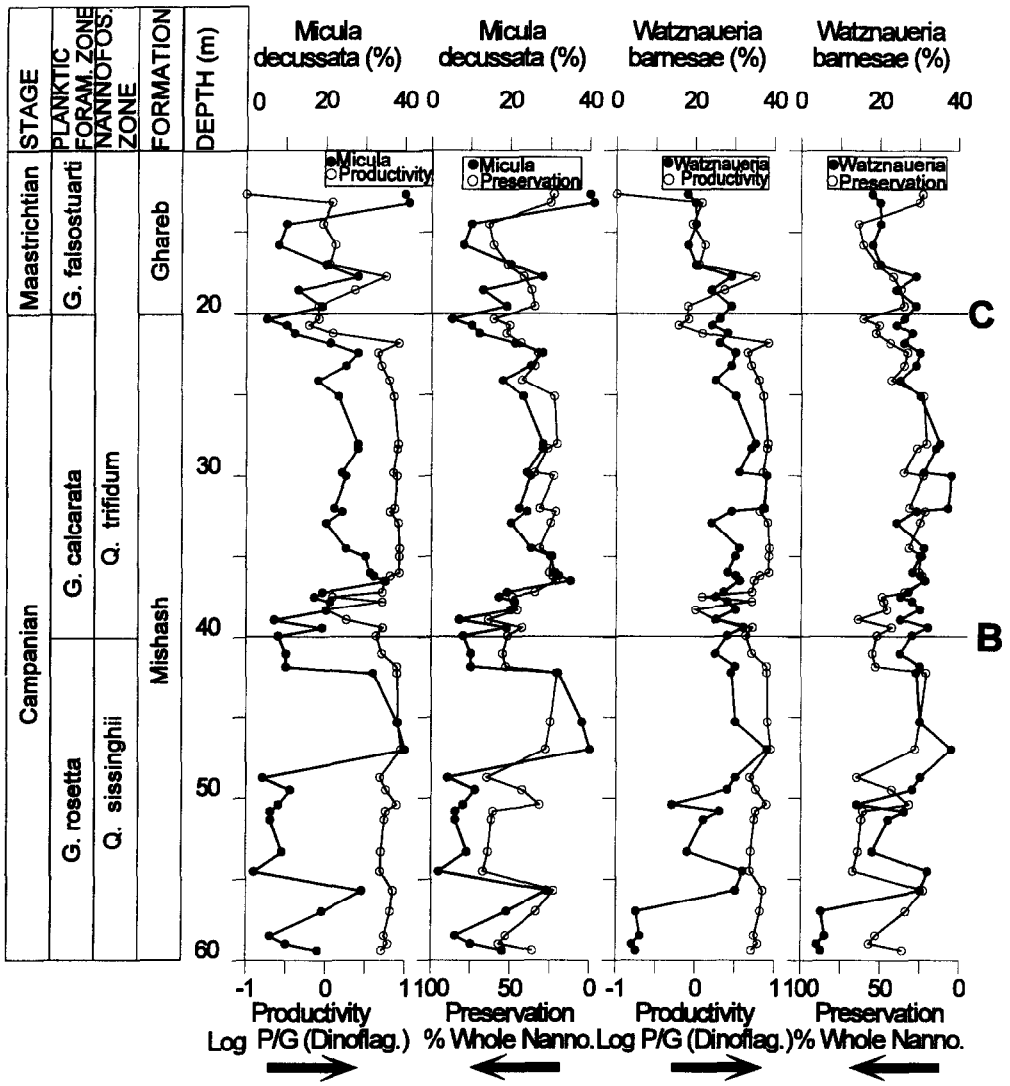


Fig. 10. Zin section: Nannofossil preservation and the distribution of *M. decussata* and *W. barnesae*.

curve of foraminifera (Fig. 9). Discrepancies in the correlation of *Micula* abundance with nannofossil and foraminifera preservation curves are explained as a result of the difference in solution -susceptibility between the two groups, as also noted by Roth and Berger (1975).

## 8. Conclusions

1. In upwelling systems, calcareous nannofossils are useful in interpreting paleoproductivity and upwelling intensity.

2. In the studied sections, nannofossil abundance and diversity attain maxima at periods when the intensity of upwelling is decreased, as indicated by the high reciprocal loadings in the Zin Basin of Nannofossils per Visual Field and Species Diversity on the high productivity indicator Factor 1. Since our data set does not include samples from oligotrophic environments, the application of these results should be regarded as limited to upwelling systems only.

3. Quantitative and statistical analyses of taxon distribution, and comparison to other independent productivity reconstructions allowed the determina-

tion of high and low productivity groups of species within the generally-productive organic-rich carbonate succession.

4. A Nannofossil Index of Productivity (NIP) was established as a sensitive index of productivity, at least in upwelling conditions: NIP is the log value of the ratio between the high- and low-productivity groups.

5. The Nannofossil Index of Productivity curves were used to correlate the studied sections and reconstruct the spatial and temporal development of productivity.

6. Inverse relationships between carbonate precipitation and organic matter preservation are reflected by their reciprocal high loadings on Factor 4 in the Zin Basin. The utility of the solution-resistant taxon *Micula decussata* as indicator of nannofossil preservation is indicated by its high loadings on Factor 2 that represents preservation. *W. barnesae* matches the productivity curves in intermediate productivity intervals. This match is not consistent with the nannofossil preservation curves.

## Acknowledgements

This research was conducted within the framework of project No. 30147 of the Geological Survey of Israel. We thank Ms. Tamara Ber (GSI) for laboratory assistance, Dr. M. Shirav (GSI) for preparing the statistical analysis, and Ms. B. Katz for text editing. Dr. J. Burnett (Univ. College, London), Dr. J. Pospichal (Florida State Univ., Tallahassee), and Dr. J. Young (Natural History Museum, London) are thanked for their useful comments on the manuscript.

## References

Ahagon, N., Tanaka, Y. and Ujiie, H., 1993. *Florisphaera profunda*, a possible nannoplankton indicator of late Quaternary changes in sea-water turbidity at the northwestern margin of the Pacific. Mar. Micropaleontol., 22: 255–273.

Almogi-Labin, A., Bein, A. and Sass, E., 1993. Late Cretaceous upwelling system along the southern Tethys margins (Israel): interrelationship between productivity, bottom-water environments and organic matter preservation: Paleoceanography, 8: 671–690.

Backman, J. and Chepstow-Lusty, A., 1993. Data report: Late Pliocene *Discoaster* abundances from ODP Hole 806C. Proc. ODP Init. Rep., 130B: 755–759.

Bartov, Y., Garfunkel, Z., Eyal, Y. and Steinitz, G., 1972. Late Cretaceous and Tertiary stratigraphy in southern Israel. Isr. J. Earth Sci., 21: 69–97.

Bein, A., Almogi-Labin, A. and Sass, E., 1990. Sulfur sinks and organic carbon relationships in Cretaceous organic-rich carbonates: implications for evaluation of oxygen-poor depositional environments. Am. J. Sci., 290: 882–911.

Bender, F., 1974. Geology of Jordan. Gebrüder Borntraeger, Berlin, 196 pp.

Bralower, T.J. and Thierstein, H.R., 1984. Low productivity and slow deep water circulation in mid-Cretaceous oceans. Geology, 12: 614–618.

Bralower, T.J. and Thierstein, H.R., 1987. Organic carbon and metal accumulation rates in Holocene and mid-Cretaceous sediments: palaeoceanographic significance. In: J. Brooks and A.J Fleet (Editors), Marine Petroleum Source Rocks. Geol. Soc. Spec. Publ., 26: 345–369.

Bralower, T.J, Arthur, M.A., Leckie, R.M., Sliter, W.V., Allard, D.J. and Schlanger, S.O., 1994. Timing and paleoceanography of oceanic dysoxia/anoxia in the Late Barremian to Early Aptian (Early Cretaceous). Palaios, 9: 335–369.

Brand, L.E., 1994. Physiological ecology of marine coccolithophores. In: A. Winter and W.G. Siesser (Editors), Coccolithophores. Cambridge Univ. Press, pp. 39–49.

Chepstow-Lusty, A. and Chapman, M., 1995. The decline and extinction of Upper Pliocene Discoasters: A comparison of two equatorial Pacific Ocean records. J. Nannoplakton Res., 17: 15–19.

Davis, J.C., 1973. Statistics and data analysis in geology. Wiley, New York, N.Y., 550.

Erba, E., Castradori, D., Guasti, G. and Ripepe, M., 1992. Calcareous nannofossils and Milankovich cycles: the example of the Albian Gault Clay Formation (southern England). Palaeogeogr., Palaeoclimatol., Palaeoecol., 93: 47–69.

Eshet, Y., Moshkovitz, S., Habib, D., Benjamini, C. and Magaritz, M., 1992. Calcareous nannofossil and dinoflagellate stratigraphy across the Cretaceous/Tertiary boundary at Hor Hahar, Israel. Mar. Micropaleontol., 18: 199–228.

Eshet, Y., Almogi-Labin, A. and Bein, A., 1994. Dinoflagellate cysts, paleoproductivity and upwelling systems: a Late Cretaceous example from Israel. Mar. Micropaleontol., 23: 231–240.

Eshet, Y. and Moshkovitz, S., 1995. Nannofossil biostratigraphy for Late Cretaceous organic-rich carbonates in Israel. Micropaleontology, 41: 321–341.

Eshet, Y., 1996. Obtaining rich nannofossil assemblages from 'barren' samples: processing organic-rich rocks in nannofossil investigations. J. Nannoplankton Res., 18: 17–21.

Flexer, A., 1968. Stratigraphy and facies development of Mount Scopus Group (Senonian–Paleocene) in Israel and adjacent countries. Isr. J. Earth Sci., 17: 85–114.

Florés, J.A., 1992. Calcareous nannofossil high-resolution quantitative analyses in the Pliocene of ODP sites 849 and 852 (Leg 138, eastern Equatorial Pacific). 4th Int. Conf. Paleoceanography, Kiel, Program & Abstracts, p. 113.

Fütterer, D., 1976. Kalkige dinoflagellaten ("calcidinelloideae") und die systematische Stellung der Thoracosphaeroidea. Neues Jahrb. Geol. Paläeontol. Abh., 151: 119–141.

Germann, K., Bock, W.D., Ganz, H., Schröter, T. and Tröger, U., 1987. Depositional conditions of Late Cretaceous phosphorites and black-shales in Egypt. Berl. Geowis. Abh., A (75.3): 629–668.

Giraudeau, J., 1992. Distribution of recent nannofossils beneath the Benguela system: southwest African continental margin. Mar. Geol., 108: 219–237.

Girgis, M.H., 1989. A morphometric analysis of the *Arkhangelskiella* group and its stratigraphical and palaeoenvironmental importance. In: J. Crux and S. van Heck, (Editors), Nannofossils and their Applications. Ellis Horwood Ltd, Chichester, pp. 327–339.

Glenn, C.R., 1990. Depositional sequences of the Duwi, Sibaiya and Phosphate Formations, Egypt: phosphogenesis and glauconitization in a Late Cretaceous epeiric sea. In: A.J.G. Notholt and I. Jarvis (Editors), Phosphorite Research and Development. Geol. Soc. Spec. Publ., 52: 205–222.

Gvirtzman, G., Almogi-Labin, A., Moshkovitz, S., Lewy, Z., Honigstein, A. and Reiss, Z., 1989. Upper Cretaceous high-resolution multiple stratigraphy, northern margin of the Arabian platform, central Israel. Cretaceous Res., 10: 107–135.

Hill, M.E., 1975. Selective dissolution of mid-Cretaceous (Cenomanian) calcareous nannofossils. Micropaleontology, 21: 227–235.

Jimenez, R., 1981. Composition and distribution of phytoplankton in the upwelling system of the Galapagos Islands. In: F.A. Richards (Editor): Coastal Upwelling. Am. Geophys. Union, pp. 327–338.

Lamolda, M.A., Gorostidi, A. and Paul, R.C., 1992. Quantitative estimates of calcareous nannofossil changes across the Plenus Marls (latest Cenomanian), Dover, England: implications for the generation of the Cenomanian–Turonian boundary event. Cretaceous Res. 15: 143–164.

Lewis, J., Dodge, J.D. and Powell, A.J., 1990. Quaternary dinoflagellate cysts from the upwelling system offshore Peru, Hole 686B, ODP Leg 112. In: E.R. Suess, R. von Huene et al., Proc. ODP Sci. Results, 112: 323–328.

Lewy, Z., 1990. Transgressions, regressions and relative sea level changes on the Cretaceous shelf of Israel and adjacent countries: A critical evaluation of Cretaceous global sea level correlations. Palaeoceanography, 5: 619–637.

Matter, A., Douglas, R.G. and Perch-Nielsen, K., 1975. Fossil preservation, geochemistry and diagenesis of pelagic carbonates from Shatsky Rise, Northwest Pacific. In: R. Moberlly (Editor), Init. Rep. DSDP, 32: 891–921.

McIntyre, A., and Bé, A.W.H., 1967. Modern coccolithophoridae of the Atlantic Ocean — I. Placoliths and cyrtoliths. Deep-Sea Res., 14: 561–597.

Molfino, B. and McIntyre, A., 1990. Precessional forcing of nutricline dynamics in the Equatorial Atlantic. Science, 249: 766–769.

Moshkovitz, S., Ehrlich, A. and Soudri, D., 1983. Siliceous microfossils of the Upper Cretaceous Mishash Formation, Central Negev, Israel. Cretaceous Res., 4: 173–194.

Okada, H. and McIntyre, A., 1979. Seasonal distribution of modern coccolithophores in the western North Atlantic Ocean. Mar. Biol. 54: 319–328.

Pedersen, T.F. and Calvert, S.E., 1990. Anoxia vs. productivity: what controls the formation of organic carbon-rich sediments and sedimentary rocks? Am. Assoc. Petrol. Geol. Bull., 74: 454–466.

Powell. A.J., Dodge, J.D. and Lewis, J., 1990. Late Neogene to Pleistocene palynological facies of the Peruvian continental margin upwelling, Leg 112. In: E.R. Suess et al., Proc. ODP Sci. Results, 112: 297–321.

Reid, F.M.H., 1980. Coccolithophorids in the North Pacific Central Gyre with notes on their vertical and seasonal distribution. Micropaleontology, 26: 151–176.

Reid, F.M.H., Stewart, E., Eppley, R.W. and Goodman, D., 1978. Spatial distribution of phytoplankton species in chlorophyll maximum layers off southern California. Limnol. Oceanogr., 23: 219–226.

Reiss, Z., Almogi-Labin, A., Honigstein, A., Lewy, Z., Lipson-Benitah, S., Moshkovitz, S. and Zaks, Y., 1985. Late Cretaceous multiple stratigraphic framework of Israel. Isr. J. Earth Sci., 34: 147–166.

Reiss, Z., 1988. Assemblages from a Senonian high productivity sea. Rev. Paléobiol., Vol. Spec., 2 (Benthos 86′): 323–332.

Roth, P.H., 1978. Calcareous nannoplankton biostratigraphy and oceanography of the Northwestern Atlantic Ocean. Init. Rep. DSDP, 44: 731–759.

Roth, P.H., 1981. Mid-Cretaceous calcareous nannoplankton from the Central Pacific: implications for paleoceanography. Init. Rep. DSDP, 62: 471–489.

Roth, P.H., 1983. Calcareous nannofossils in mid-Cretaceous black shale cycles from the Atlantic and Pacific: effects of diagenesis. Eos, 64: 733–734.

Roth, P.H., 1994. Distribution of coccoliths in oceanic sediments. In: A. Winter and W.G Siesser (Editors), Coccolithophores. Cambridge Univ. Press, pp. 199–218.

Roth, P.H. and Berger, H., 1975. Distribution and dissolution of coccoliths in the South and Central Pacific. In: W.V. Sliter, A.W.H. Bé and W. Berger (Editors), Dissolution of Deep Sea Carbonates. Cushman Found. Foraminiferal. Res., Spec. Publ. 13: 87–113.

Roth, P.H. and Bowdler, J.L., 1981. Middle Cretaceous calcareous nannoplankton biogeography and oceanography of the Atlantic Ocean. Soc. Econ. Paleontol. Miner., Spec. Publ., 32: 517–546.

Roth, P.H. and Krumbach, K.R., 1986. Middle Cretaceous calcareous nannofossil biogeography and preservation in the Atlantic and Indian Oceans: implications for paleoceanography. Mar. Micropaleontol., 10: 235–266.

Rojas de Mandiola, B., 1981. Seasonal phytoplankton distribution along the Peruvian coast. In: F.A. Richards (Editor), Coastal Upwelling, Am. Geophys. Union, pp. 348–356.

Schlanger, S.O., Douglas, R.G. and Lancelot, Y., 1973. Fossil preservation and diagenesis of pelagic carbonates from the Magellan Rise, central North Pacific Ocean. In: E.L Winterer et al. (Editors), Init. Rep. DSDP, 17: 407–427.

Shemesh, A. and Kolodny, Y., 1988. Oxygen isotope variations in phosphorites from the southeastern Tethys. Isr. J. Earth Sci., 37: 1–15.

Sissingh, W., 1977. Biostratigraphy of Cretaceous calcareous

nannoplankton. Geol. Mijnbouw, 57: 433–440.

Thiede, J. and Jünger, B., 1992. Faunal and floral indicators of ocean coastal upwelling (NW African and Peruvian continental margins). In: C.P. Summerhayes, W.L. Prell and K.C. Emeis (Editors), Upwelling Systems: Evolution Since the Early Miocene. Geol. Soc., London, pp. 47–76.

Thierstein, H., 1980. Selective dissolution of Late Cretaceous and earliest Tertiary calcareous nannofossils: experimental evidence. Cretaceous Res., 2: 165–176.

Thunell, R.C and Sautter, L.R., 1992. Planktonic foraminiferal, faunal and stable isotope indices of upwelling: a sediment-trap study in the San Pedro Basin, Southern California Bight. In: C.P. Summerhayes, W.L. Prell and K.C. Emeis (Editors), Upwelling Systems: Evolution Since the Early Miocene. Geol. Soc., Spec. Publ., 64: 77–91.

Watkins, D.K., 1989. Nannoplankton productivity fluctuations and rhythmically-bedded pelagic carbonates of the Greenhorn Limestone (Upper Cretaceous). Palaeogeogr., Palaeoclimatol., Palaeoecol., 74: 75–86.

Winter, A., 1985. Distribution of living coccolithophores in the California Current system, southern California borderland. Mar. Micropaleontol., 9: 385–393.

Winter, A., Reiss, Z. and Luz, B., 1979. Distribution of living coccolithophore assemblages from the Gulf of Elat (Aqaba). Mar. Micropaleontol., 4: 197–223.

Winter, A., Jordan, R.W. and Roth, P.H., 1994. Biogeography of living coccolithophores in ocean waters. In: A. Winter and W.G Siesser (Editors), Coccolithophores. Cambridge Univ. Press, pp. 161–177.

Wise, S.W., 1982. Calcareous nannofossils: an update. Third Am. Paleontol. Conf., Proc., 1: 588a–588j.

Young, J.R., 1987. Possible functional interpretation of coccolith morphology. Abh. Geol. B.-A., 39: 305–313.

Young, J.R., 1994. Functions of coccoliths. In: A. Winter and W.G Siesser (Editors), Coccolithophores. Cambridge Univ. Press, pp. 63–82.

Ziveri, P., Thunell, R.C. and Rio, D., 1995. Export production of coccolithophores in an upwelling region: results from San Pedro Basin, Southern California borderlands. Mar. Micropaleontol., 24: 335–358.